CHEMISTRY
A EUROPEAN JOURNAL

DOI: 10.1002/chem.200902342

Positionally Isomeric Organic Gelators: Structure–Gelation Study, Racemic versus Enantiomeric Gelators, and Solvation Effects

Vesna Čaplar, Leo Frkanec, Nataša Šijaković Vujičić, and Mladen Žinić*[a]

Abstract: Low molecular weight gelator molecules consisting of aliphatic acid, amino acid (phenylglycine), and ω-aminoaliphatic acid units have been designed. By varying the number of methylene units in the aliphatic and ω-aminoaliphatic acid chains, as defined by descriptors *m* and *n*, respectively, a series of positionally isomeric gelators having different positions of the peptidic hydrogen-bonding unit within the gelator molecule has been obtained. The gelation properties of the positional isomers have been determined in relation to a defined set of twenty solvents of different structure and polarity and analyzed in terms of gelator versatility (G_{ver}) and effectiveness (G_{eff}). The results of gelation tests have shown that simple synthetic optimizations of a "lead gelator molecule" by variation of *m* and *n*, end-group polarity (carboxylic acid versus sodium carboxylate), and stereochemistry (racemate versus optically pure form) allowed the identification of gelators with tremendously improved versatility (G_{ver}) and effectiveness (G_{eff}). Dramatic differences in G_{eff} values of up to 70 times could be observed between pure racemate/enantiomer pairs of some gelators, which were manifested even in the gelation of very similar solvents such as isomeric xylenes. The combined results of spectroscopic (^{1}H NMR, FTIR), electron microscopy (TEM), and X-ray diffraction studies suggest similar organization of the positionally isomeric gelators at the molecular level, comprising parallel β-sheet hydrogen-bonded primary assemblies that form inversed bilayers at a higher organizational level. Differential scanning calorimetry (DSC) studies of selected enantiomer/racemate gelator pairs and their *o*- and *p*-xylene gels revealed the simultaneous presence of different polymorphs in the racemate gels. The increased gelation effectiveness of the racemate compared to that of the single enantiomer is most likely a consequence of its spontaneous resolution into enantiomeric bilayers and their subsequent organization into polymorphic aggregates of different energy. The latter determine the gel fiber thickness and solvent immobilization capacity of the formed gel network.

Keywords: enantiomers · fatty acids · gelation · racemates · self-assembly

Introduction

The gelation of water and various organic fluids by low molecular weight organic gelators, giving in most cases thermally reversible gels, has emerged as a fascinating supramolecular phenomenon.[1] The topic has received much attention due to potential applications in many areas, such as in the preparation of viscoelastic materials, the cosmetics industry, the design of drug delivery systems and sensors, tissue engineering, food processing, and pharmacology.[2] Organogelators are molecules capable of self-assembling into long, fibrous structures of nanosized diameters through highly specific noncovalent interactions such as hydrogen bonding, van der Waals, π-stacking, electrostatic, and charge-transfer interactions.[3] Noncovalent cross-links between the nanofibers and/or mechanical entanglements create a three-dimensional network, which entraps the solvent inside the interstices leading to gelation and loss of fluidity of the system. Hence, the observation of gelation indicates the occurrence of the self-assembly of gelator molecules and represents a macroscopic manifestation thereof. The basic structural requirement for a molecule to exhibit gelation properties is its self-complementarity and capability of undergoing unidirectional self-assembly into fibrous aggregates instead of dissolution or crystallization.[3] However, despite the considerable advances in the understanding of gelation as a supramolec-

[a] Dr. V. Čaplar, Dr. L. Frkanec, N. Š. Vujičić, Prof. Dr. M. Žinić
Division of Organic Chemistry and Biochemistry
Laboratory for Supramolecular and Nucleoside Chemistry
Ruđer Bošković Institute, P.O.B. 180, 10002 Zagreb (Croatia)
Fax: (+385) 1-4680-195
E-mail: zinic@irb.hr

Supporting information for this article is available on the WWW under http://dx.doi.org/10.1002/chem.200902342.

ular phenomenon, it is still scarcely possible to predict its appearance on the basis of structural characteristics of a candidate molecule and it is even more difficult to predict which solvents might be gelled and with what degree of efficiency.[4] Hence, structure–gelation relationship studies based on systematic structural variations of a selected "lead gelator molecule", followed by a determination of gelation properties, the morphological characteristics of the gel fibers, and the self-assembly motifs of its structural variants, would seem necessary. Such studies may provide a deeper understanding of the gelation mechanism and also shed more light on the role of the solvent as the second supramolecular partner of each gelation system.[3a,5]

In our earlier work on low molecular weight gelators of water and organic solvents, we prepared chiral gelators constructed from 11-aminoundecanoic, lauric, and amino acid units.[6] This combination of structural fragments was assumed to be favorable for gelation.

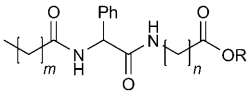

m = 10, *n* = 10, R = H
m = 10, *n* = 10, R = Na

Indeed, some of the representatives of this series in the free-acid or sodium carboxylate forms exhibited excellent gelation properties, being capable of gelling both highly polar solvents (water, DMSO) as well as highly lipophilic solvents, including some common hydrocarbon fuels (gasoline, diesel). Spectroscopic studies revealed that intermolecular hydrogen-bonding interactions between the peptidic and carboxylic acid units are involved in the stabilization of the gel assemblies. For gelators with terminal sodium carboxylate groups, an additional strong stabilization of the aggregates was attributed to the electrostatic and ion-dipole interactions between the carboxylate moieties and the sodium cations.[6d]

As a further step in the investigation of this class of versatile gelators, we decided to study their structure–gelation relationships by preparing a set of isomers with variable lengths of the terminal and carboxylic acid methylene chains. The chain lengths are defined by descriptors *m* and *n*, which correspond to the number of methylene units in the terminal and carboxylic acid chains, respectively. Keeping the sum of $m + n$ constant at 20, a set of positionally isomeric gelators was obtained, having the same hydrophilic/lipophilic balance (ratio of lipophilic and polar groups in the gelator molecule), but with variable position of the core -CONH–CHPhCONH- hydrogen-bonding unit within the main chain of the gelator molecule (Figure 1). Such positionally isomeric gelators are expected to self-assemble by using the same type of intermolecular forces (H-bonding and lipophilic alkyl chain interactions); however, the variations of alkyl chain lengths (*m* and *n*) may strongly influence their gelation properties through affecting the strength of intermolecular interactions, solubility in various solvents and their organization at the supramolecular level which could be reflected in different fiber morphology and thermal properties of gels. Besides the variation of *m* and *n*, the end-group polarity could be altered by transformation of the carboxylic acid into sodium carboxylate, and the influence of stereochemistry could be assessed by comparing the gelation properties of the racemates and optically pure forms.

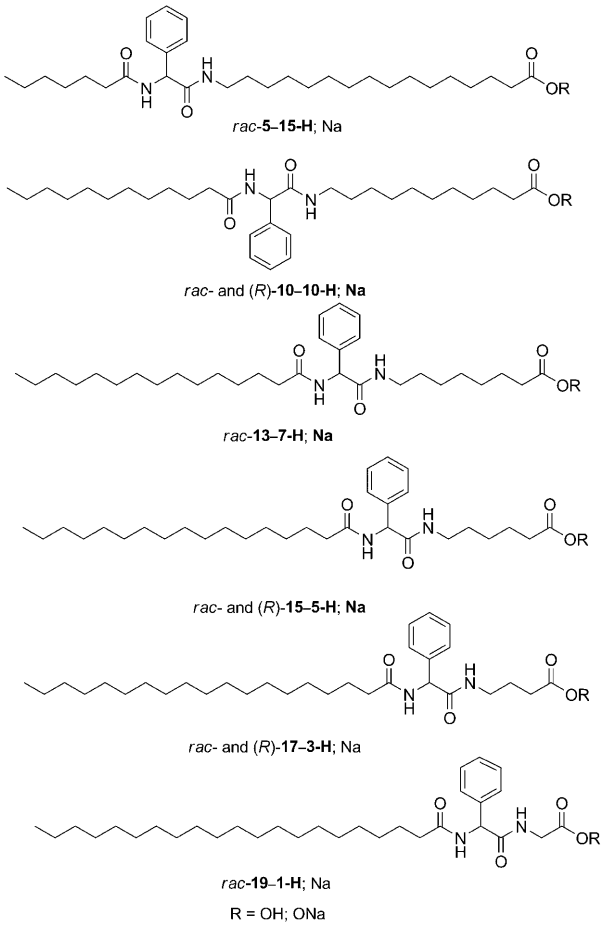

rac-**5–15-H**; Na

rac- and (*R*)-**10–10-H**; **Na**

rac-**13–7-H**; **Na**

rac- and (*R*)-**15–5-H**; **Na**

rac- and (*R*)-**17–3-H**; Na

rac-**19–1-H**; Na

R = OH; ONa

Figure 1. Positionally isomeric carboxylic acid gelators with varying numbers of methylene units *m* and *n* in their terminal and carboxylic acid alkyl chains, respectively. The isomers are denoted as ***m*-*n*-H** or ***m*-*n*-Na** using the *m* and *n* descriptors.

In this work, we report on the synthesis of six positionally isomeric free-acid and sodium salt gelators in racemic and optically pure forms and present the results of a comparative gelation study employing a selected set of twenty solvents of different structures and polarities. The gelation properties of each positional isomer have been analyzed in terms of its versatility (G_{ver}) and effectiveness (G_{eff}). G_{ver} indicates the number of different solvents from the defined set that could be gelled by the tested positional isomer, which in turn describes its capacity to gel solvents of different structure and polarity. G_{eff} is expressed in mL of the tested solvent and shows how great a volume could be immobilized by 10 mg of the tested positional isomer. Hence, the G_{eff} values reveal the gelation capacity of each positional isomer toward the selected solvent.

Herein, we demonstrate that simple synthetic optimizations of a "lead gelator molecule" by the variation of alkyl chain lengths (m and n), end-group polarity (carboxylic acid versus sodium carboxylate), and stereochemistry (racemate versus optically pure form) can lead to the identification of gelators with tremendously improved versatility (G_{ver}) and effectiveness (G_{eff}). The described gelator optimization approach may be of great benefit in the search for highly efficient gelators of a targeted solvent. We also show that dramatic differences in G_{eff} values of up to 70 times could be observed even in the gelation of very similar solvents such as isomeric xylenes. The combined results of spectroscopic (^{1}H NMR, FTIR), electron microscopy (TEM), X-ray diffraction, and differential scanning calorimetry (DSC) studies suggest that the observed G_{eff} differences are not the consequence of different organization of the positional isomers at the molecular level, which was found to be very similar in each case, but more likely the consequence of different organization at the supramolecular level, affected by specific solvation effects, the latter depending even on the solvent structure, as found in the gelation of isomeric xylenes.

Results and Discussion

Synthesis: A set of candidate gelator molecules was prepared, each containing a core racemic or optically active phenylglycine fragment, by varying the number of methylene units in the terminal (m) and interposed (n) aliphatic chains (Figure 1). The general synthetic route involved coupling of an *N*-protected racemic or (*R*)-phenylglycine reactive ester with a selected ω-aminoalkyl carboxylic acid methyl ester, followed by deprotection and acylation of the phenylglycine alkylamide with an appropriate acyl chloride (Scheme 1). The obtained methyl esters were hydrolyzed to free acids or sodium salts. Methyl esters of glycine, 4-aminobutyric acid, and 6-aminohexanoic acid are commercially available; methyl esters of 8-aminooctanoic acid and 11-aminoundecanoic acid were prepared by esterification of the corresponding acids using MeOH and $SOCl_2$.

The methyl ester of 16-aminohexadecanoic acid was prepared by initial esterification of 16-bromohexadecanoic acid. Subsequent substitution of the bromo substituent by an azido group and hydrogenolysis of the azido derivative gave methyl ω-aminohexadecanoate, which was used in the preparation of compounds with $m=5$, $n=15$. *N*-Heptanoylphenylglycine was prepared by acylation of phenylglycine with heptanoyl chloride and then coupled with methyl 16-aminohexadecanoate under activation by Ph_3P, CCl_4, and Et_3N (Scheme 2). Subsequent alkaline hydrolysis of the ester gave the sodium salt **15–5-Na** and after acidification the free acid **15–5-H**.

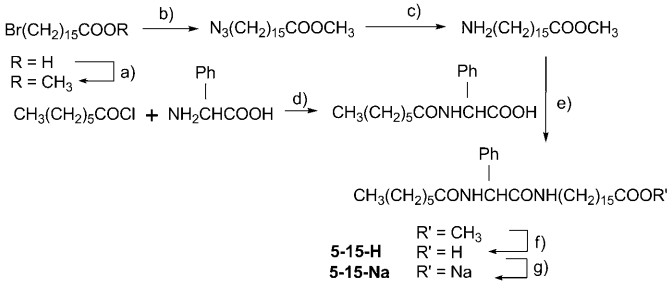

Scheme 2. a) CH_3OH, H_2SO_4; b) NaN_3/MeCN; c) H_2-Pd/MeOH; d) NaOH/H_2O; e) Ph_3P, Et_3N, CCl_4/MeCN; f) NaOH, HCl; g) NaOH.

In the case of the long terminal alkyl chain derivative **19–1-H**, the $m=19$ fragment was prepared starting from 1-bromoeicosane, the bromo substituent of which was replaced by cyanide and then the cyano derivative was hydrolyzed to heneicosanoic acid (Scheme 3). The synthetic route using methyl phenylglycylglycinate for the preparation of the phenylglycylglycine derivative ($n=1$) failed due to formation of the respective diketopiperazine. Therefore, the glycine fragment had to be introduced in the last step. Heneicosanoic acid was activated by succinimide ester formation and coupled with phenylglycine methyl ester; this intermediate was hydrolyzed and finally coupled with glycine methyl ester under activation with Ph_3P, CCl_4, and Et_3N. The resulting ester was hydrolyzed to give the corresponding free-acid and sodium salt derivatives.

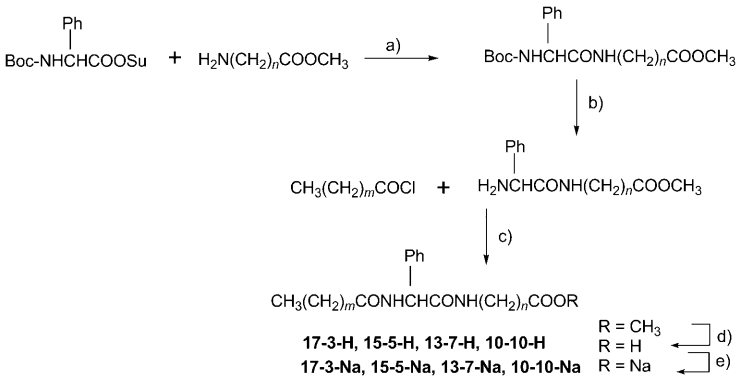

Scheme 1. a) Et_3N/dioxane; b) TFA/CH_2Cl_2; c) Et_3N/CH_2Cl_2; d) NaOH, H^+; e) NaOH.

Gelation properties of racemic positionally isomeric carboxylic acid gelators: Racemic free-acid derivatives **19–1-H**, **17–3-H**, **15–5-H**, **13–7-H**, **10–10-H**, and **5–15-H** were tested with regard to their gelation properties toward water and selected polar and apolar organic solvents (Table 1 and Figure 2). However, all of the tested free-acid gelators were insoluble in water so that no hydrogelation was observed. Only the posi-

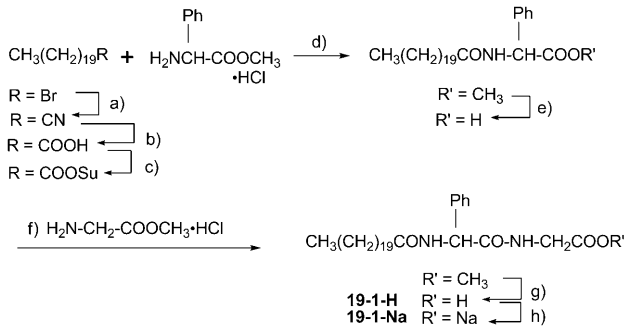

Scheme 3. a) KCN/DMF, b) 50% H_2SO_4; c) HOSu, DCC/dioxane; d) Et_3N/dioxane; e) NaOH/MeOH, H^+; f) Ph_3P, Et_3N, CCl_4/MeCN; g) NaOH, MeOH, H^+; h) NaOH.

using the public domain software ALOGPS 2.1.[7] The average log*P* values showed all of the positionally isomeric gelators to be highly lipophilic compounds, albeit with slightly different log*P* values that decrease with decreasing *m* and increasing *n* descriptors (**19–1-H**: 8.39, **17–3-H**: 8.16, **15–5-H**: 8.05, **13–7-H**: 8.04, **10–10-H**: 8.03, and **5–15-H**: 7.93). Hence, the more lipophilic positional isomers with $m=19$, 17, 15, and 13 appear to be insufficiently soluble in highly polar and hydrogen-bond competitive solvents (water, DMSO, DMF, EtOH, acetone, EtOAc) or tend to crystallize from hot solutions, presumably due to inefficient solvation of their long terminal alkyl chains. In addition, the extensive gelator–solvent hydrogen bonding competes with the self-assembly process, so that crystallization becomes a favored process. The presence of shorter terminal chains in **10–10-H** and **5–15-H** ($m=10$, 5) enables their dissolution in highly polar DMSO and DMF or results in crystallization from solutions in less polar and apolar solvents. However, apolar solvents are capable of efficiently competing with the self-assembly of **10–10-H** and **5–15-H** due to weaker intermolecular lipophilic interactions between their shorter alkyl chains. The more lipophilic isomers **19–1-H**, **17–3-H**, and **15–5-H** are sufficiently soluble in lipophilic aromatic solvents, decalin, and hydrocarbon fuels, which also favor strong intermolecular hydrogen bonding, so that the self-assembly leading to gelation is strongly favored.

It can be noted, however, that **19–1-H**, the most lipophilic of the positional isomers, is less versatile ($G_{ver}=5$) than **17–3-H** and **15–5-H** ($G_{ver}=9$ and 10), both of which are slightly less lipophilic than **19–1-H** but capable of gelling a wider range of lipophilic aliphatic and aromatic solvents and even tional isomers **17–3-H** and **15–5-H** with longer terminal alkyl chains ($m=17$, 15) gelled small volumes of DMSO to give milky opaque gels, while the other isomers were soluble. DMF and EtOH were not gelled, nor were other solvents of medium polarity. It was observed that **17–3-H** crystallized from acetone, ethyl acetate, acetonitrile, and cyclohexane to produce a network of very long, microcrystalline fibers resembling cotton-wool, which was capable of trapping large volumes of solvents. The results of gelation experiments collected in Table 1 show that some of the investigated positional isomers exhibited excellent gelation of aromatic solvents, decalin, and two common hydrocarbon fuels, while others were incapable of gelling any of the twenty tested solvents. The positional isomers **5–15-H**, **10–10-H**, and **13–7-H** with shorter terminal chains ($m=5$, 10, and 13) and longer carboxylic acid chains ($n=15$, 10, and 7) lacked gelation ability toward both polar and apolar solvents, although **13–7-H** was capable of gelating a very small volume of tetralin (Table 1, Experimental Section, and Figure 2).

Table 1. Gelation efficiencies (G_{eff}, mL) and MGC values (in parentheses; 10^{-3} mol dm^{-3}) of racemic acid gelators **19–1-H**, **17–3-H**, **15–5-H**, **13–7-H**, **10–10-H**, and **5–15-H**.

Solvent	**19–1-H**	**17–3-H**	**15–5-H**	**13–7-H**	**10–10-H**	**5–15-H**
water	ins.	ins.	ins.	ins.	ins.	ins.
DMSO	t.v.s.	0.7[a] (27.6)	0.5[a] (38.7)	fl.	sol.	sol.
DMF	cr.	cr.	fl.	fl.	sol.	sol.
EtOH	cr.	cr.	cr.	fl.	cr.	sl. sol.
acetone	ins.	c.w. (6.45)	fl.	cr.	cr.	sl. sol.
EtOAc	ins.	c.w. (6.45)	fl.	cr.	cr.	cr.
MeCN	ins.	c.w. (6.91)	cr.	cr.	cr.	cr.
THF	cr.	cr.	sol.	sol.	sol.	sol.
CH_2Cl_2	ins.	ins.	ins.	sol.	sol.	sol.
CCl_4	fl.	sl. sol. fl.	cr.	sol.	–	w.
cyclohexane	fl.	c.w. (9.68)	cr.	emuls.		t.v.s.
benzene	fl.	11.8[a] (1.64)	4.4[a] (4.40)	sol.	sol.	ins.
toluene	31.5[b] (0.61)	8.5[b] (2.28)	3.5[a] (5.53)	cr.	cr.	ins.
o-xylene	9.3[b] (2.08)	26.7[b] (0.72)	5.9[a] (3.28)	w.	cr.	–
m-xylene	1.4[a] (13.8)	15.0[b] (1.19)	6.0[b] (3.22)	w.	cr.	–
p-xylene	1.8[a] (10.7)	5.8[b] (3.34)	14.7[b] (1.32)	w.	cr.	ins.
tetralin	8.6[b] (2.25)	10.2[b] (1.90)	4.5[b] (4.30)	32.2[b]	t.v.s.	ins.
decalin	fl.	fl.	2.6[a] (7.44)	w.	t.v.s.	ins.
gasoline	w.	2.0[a] (9.68)	11.6[a] (1.67)	ins.	ins.	ins.
diesel	fl.	1.0[a] (19.3)	2.0 (9.68)[b]	ins.	ins.	ins.

[a] Colorless opaque gel. [b] Colorless transparent gel. Abbreviations: t.v.s. = turbid viscous solution, fl. = flocculent precipitate, cr. = crystals, ins. = insoluble, sol. = soluble, w. = wax-like precipitate, c.w. = cotton wool-like precipitate.

Racemic **17–3-H** and **15–5-H** ($G_{ver}=9$ and 10) appeared to be the most versatile gelators among the tested positional isomers, being capable of gelling nine and ten of the twenty solvents tested, including two common hydrocarbon fuels (gasoline, diesel). The isomer **19–1-H**, with the longest terminal alkyl chain ($m=19$) and the shortest carboxylic acid chain ($n=1$), proved to be much less versatile, displaying a G_{ver} value of only 5. To account for the observed differences in G_{ver} between the positional isomers, their relative lipophilicities were estimated by calculation of average log*P* values

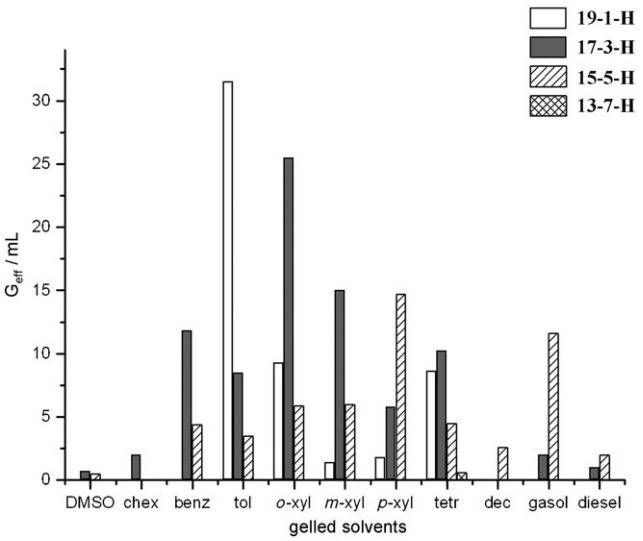

Figure 2. Gelation efficiencies, G_{eff}, of racemic **19–1-H**, **17–3-H**, **15–5-H**, and **13–7-H** for selected solvents.

a small volume of highly polar DMSO. It should also be noted that **15–5-H**, **13–7-H**, **10–10-H**, and **5–15-H**, despite having very similar average log*P* values, displayed very different G_{ver} values (**15–5-H**: $G_{ver}=10$, **13–7-H**: $G_{ver}=1$, **10–10-H** and **5–15-H**: no gelation). Hence, there is no simple relationship between the lipophilicity of a gelator and its versatility. Spectroscopic and powder XRD investigations (vide infra) suggest similar organization of the positionally isomeric gelators at the molecular level, forming assemblies stabilized by intermolecular hydrogen bonding and lipophilic interactions between aliphatic chains. As recently reported by van Esch et al.,[8] the contributions of lipophilic and hydrogen-bonding interactions to the overall stabilization of gel assemblies are different in solvents of different polarities. In polar and hydrogen-bonding competitive solvents, lipophilic interactions usually provide the dominant contribution, while in lipophilic solvents hydrogen bonding provides the major stabilizing contribution. Hence, it can be concluded that the versatility of a gelator depends in part on gelator–solvent interactions that determine its solubility in solvents of different polarity, but also on the interplay of contributions from lipophilic and hydrogen-bonding interactions, which should provide sufficient stability of the assemblies in solvents of different polarities.

Figure 2 shows that the racemic positionally isomeric gelators exhibit large differences in gelled volumes of the same solvent, defined here as gelator effectiveness (G_{eff}). Toluene is by far the most efficiently gelled by the most lipophilic **19–1-H** ($G_{eff}=31.5$ mL) compared to the less lipophilic **17–3-H** ($G_{eff}=8.5$ mL) and **15–5-H** ($G_{eff}=3.5$ mL); thus, **19–1-H** is a four and nine times more efficient gelator of toluene than the positionally isomeric **17–3-H** and **15–5-H**, respectively. Since the similar average log*P* values calculated for the positional isomers imply that they should have similar solubilities in toluene, they cannot account for the different G_{eff} values. It is particularly surprising that **19–1-H**, **17–3-H**, and **15–5-H** also exhibited very different G_{eff} values in the gelation of the isomeric xylenes, with these solvents having very similar physical properties. For *o*-xylene, the obtained G_{eff} values were: **19–1-H**: 9.3 mL, **17–3-H**: 26.7 mL, and **15–5-H**: 5.9 mL, making **17–3-H** the most efficient gelator of this solvent. The same gelator also proved to be the most efficient in the gelation of *m*-xylene. However, **15–5-H** showed a much higher G_{eff} value (14.7 mL) for *p*-xylene compared to those of **19–1-H** ($G_{eff}=1.8$ mL) and **17–3-H** ($G_{eff}=5.8$ mL).

Gelation of isomeric xylenes: Recently, Smith and Miravet[5a] showed that the efficacies of members of their class of toluene gelators were dependent on the solubility of gelator assemblies in this solvent. They presented convincing evidence that the aggregation behavior of these gelators is cooperative[9] and that the alternative isodesmic model,[10] in which there is a continuous distribution of monomers and oligomers, is not valid. Therefore, gelator molecules are distributed between a solid-like gel network (c_{crit}), in which they cannot be observed by ^{1}H NMR, and dissolved NMR-observable gelator assemblies (c_{diss}) present in the immobilized solvent. Hence, the experimentally determined minimal gelation concentration (MGC) actually represents the sum of c_{crit} and c_{diss}. When c_{diss} is equal to zero, c_{crit} corresponds to the minimal gelator concentration sufficient to immobilize the relevant volume of a solvent. It was also shown that the saturation point in the gel-to-sol transition diagrams was determined by c_{diss}, as our group found earlier for other types of gelators.[11] Hence, for gels containing a significant concentration of dissolved gelator assemblies (significant c_{diss}), the experimentally determined MGC is higher to compensate for these. According to these results, higher experimentally determined MGC values should correspond to lower gelator effectiveness G_{eff} due to higher solubility of gelator assemblies (c_{diss}). In an attempt to explain the large differences in G_{eff} found for **19–1-H**, **17–3-H**, and **15–5-H** in the gelation of isomeric xylenes as a consequence of different c_{diss}, we assumed that the solubilities of the gelator assemblies should depend on the relative lipophilicities of the positionally isomeric gelators. Hence, the most lipophilic gelator should also give the most soluble assemblies (the highest c_{diss}) in the specified solvent and consequently should be the least effective gelator.[12] The relationship between the calculated average log*P* values of the gelators and the experimentally determined G_{eff} values for toluene and isomeric xylene gels is shown in Figure 3. In marked contrast to the above predictions, **19–1-H**, as the most lipophilic gelator (average log*P* 8.39), showed the highest G_{eff} of 31.5 mL in the gelation of toluene compared to the values for the less lipophilic **17–3-H** and **15–5-H**. The relationships between the lipophilicities of **19–1-H**, **17–3-H**, and **15–5-H** and their G_{eff} values determined for *o*-, *m*-, and *p*-xylene gels are also at variance with the prediction that the highest G_{eff} should be observed for the least lipophilic gelator, this only being

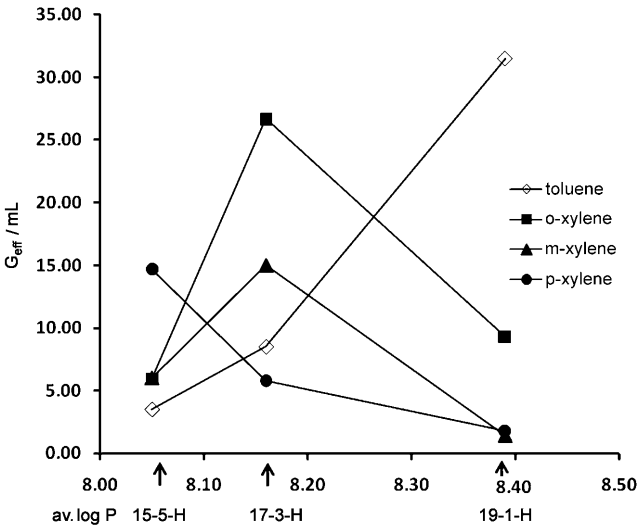

Figure 3. Graphical presentation of G_{eff} values determined for toluene, and *o*-, *m*-, and *p*-xylene gels of **19–1-H**, **17–3-H**, and **15–5-H**, with their average log*P* values indicated by arrows.

true for *p*-xylene gels, in which case the most lipophilic **19–1-H** showed the lowest effectiveness.

Apparently, the observed large G_{eff} differences among the positionally isomeric gelators in the gelation of toluene and *o*-, *m*-, and *p*-xylenes, solvents of very similar lipophilicities, cannot be explained by considering only the solubility of the gelator assemblies. Rather, the observed gelator effectiveness seems to be dominated by specific solvation effects involved in the self-assembly processes at different levels of supramolecular organization. Recently, Meijer et al.[3a] presented convincing evidence that co-organization of solvent at the periphery of the gel aggregates plays a direct role in the assembly process, even during the formation of pre-aggregates. The influence of solvent structure on the length of the aggregates was clearly demonstrated.

Hence, in the case of the isomeric xylenes, which have very similar physical properties, the structure of the solvent is likely to influence the self-assembly and ultimately determine the gel fiber morphology.[13] Evidence has also been provided that a gel network consisting of thinner and flexible fibers has higher solvent immobilization capacity than a network composed of thick and rigid fibers.[14] This can be explained by the fact that the immobilization of solvent is predominantly due to capillary forces, which are stronger for smaller network compartments. Consequently, the specific solvation effects exhibited by structurally different isomeric xylenes may stem from the formation of fibers of different morphology, which in turn give networks of variable density having different gelation capacities. It can be concluded that gelator effectiveness may in some cases be dominated by the solubility of gelator assemblies,[5a] as well as by specific solvation effects determining the fiber and network morphology and ultimately the solvent immobilization capacity.

Carboxylic acid versus sodium salt gelators: Table 2 shows the results of gelation studies with racemic sodium salt gelators **19–1-Na**, **17–3-Na**, **15–5-Na**, **13–7-Na**, **10–10-Na**, and **5–15-Na** and the same set of twenty different solvents. Generally, the salts gelled a similar set of solvents as the acid-type gelators. Ethanol and other solvents of medium polarity were not gelled by the salts nor by the acids. Considering gelator versatility (G_{ver}), **19–1-Na** appeared to be much less versatile ($G_{ver}=2$) compared to its free-acid counterpart (**19–1-H**, $G_{ver}=5$), but, in contrast, the salt was capable of gelling a small volume of DMSO, presumably due to its somewhat better solubility in this solvent. G_{ver} values (Tables 1 and 2) of **17–3-Na** ($G_{ver}=11$) and **15–5-Na** ($G_{ver}=9$) are similar to those of the free-acid gelators **17–3-H** (9) and **15–5-H** (10) and both types of gelators showed preferential gelation of lipophilic aromatic solvents. However, in contrast to **13–7-H** and **10–10-H**, which showed practically no gelation, **13–7-Na** and **10–10-Na** showed increased gelation ability towards aromatic solvents and decalin, giving G_{ver} values of 5 and 3, respectively.

Distinct differences in gelator effectiveness (G_{eff}) between the salts and the corresponding acids were observed in the gelation of selected apolar solvents. Figure 4 enables com-

Table 2. Gelation efficiencies (G_{eff}, mL) and MGC values (in parentheses; 10^{-3} mol dm^{-3}) of sodium salt gelators **19–1-Na**, **17–3-Na**, **15–5-Na**, **13–7-Na**, **10–10-Na**, and **5–15-Na**.

Solvent	**19–1-Na**	**17–3-Na**	**15–5-Na**	**13–7-Na**	**10–10-Na**	**5–15-Na**
water	t.v.s.	t.v.s.	1.0[a] (18.6)	1.4[a] (13.3)	0.8 (23.2)	t.v.s.
DMSO	2.0[a] (9.28)	t.v.s.	2.0[a] (9.28)	fl.	1.1 (16.9)	fl.
DMF	fl.	fl.	cr.	fl.	0.6 (30.9)	0.8[a] (23.2)
EtOH	cr.	cr.	cr.	cr.	cr.	ins.
acetone	ins.	ins.	ins.	ins.	ins.	ins.
EtOAc	cr.	ins.	ins.	ins.	ins.	ins.
MeCN	ins.	ins.	ins.	ins.	ins.	ins.
THF	fl.	ins.	ins.	ins.	ins.	ins.
CH_2Cl_2	ins.	ins.	ins.	ins.	ins.	ins.
CCl_4	ins.	0.9[a] (20.6)	ins.	ins.	–	ins.
cyclohexane	ins.	4.4[a] (42.2)	ins.	ins.	–	ins.
benzene	t.v.s.	5.3[b] (35.0)	ins.	ins.	ins.	ins.
toluene	2.1[b] (8.84)	2.0[b] (9.28)	6.8[b] (2.73)	ins.	ins.	ins.
o-xylene	sol.	2.2[b] (8.44)	5.8[b] (3.20)	0.7[b] (26.5)	w.	1.2[b] (15.5)
m-xylene	t.v.s.	2.1[b] (8.84)	2.1[b] (8.84)	1.6[b] (11.6)	w.	w.
p-xylene	t.v.s.	20.6[b] (0.90)	4.5[b] (4.12)	4.3[b] (4.32)	16.1 (1.15)	ins.
tetralin	t.v.s.	7.9[b] (2.35)	8.2[b] (2.26)	7.3[b] (2.54)	12.0 (1.55)	ins.
decalin	fl.	1.5[b] (12.4)	17.0[b] (1.09)	0.7[a] (24.7)	18.0 (1.03)	ins.
gasoline	t.v.s.	2.1[b] (8.84)	ins.	ins.	ins.	ins.
diesel	w.	3.4[b] (5.46)	2.8[b] (6.63)	ins.	ins.	ins.

[a] Colorless opaque gel, [b] Colorless transparent gel. Abbreviations: t.v.s. = turbid viscous solution, fl. = flocculent precipitate, cr. = crystals, ins. = insoluble, sol. = soluble, w. = wax-like precipitate.

parison of the G_{eff} values of the free-acid and sodium salt gelators. The acid gelator **19–1-H** (light-blue bar) displayed a 15 times higher G_{eff} (31.5 mL) for toluene than the corresponding sodium salt (**19–1-Na**, red bar, $G_{eff}=2.1$ mL).

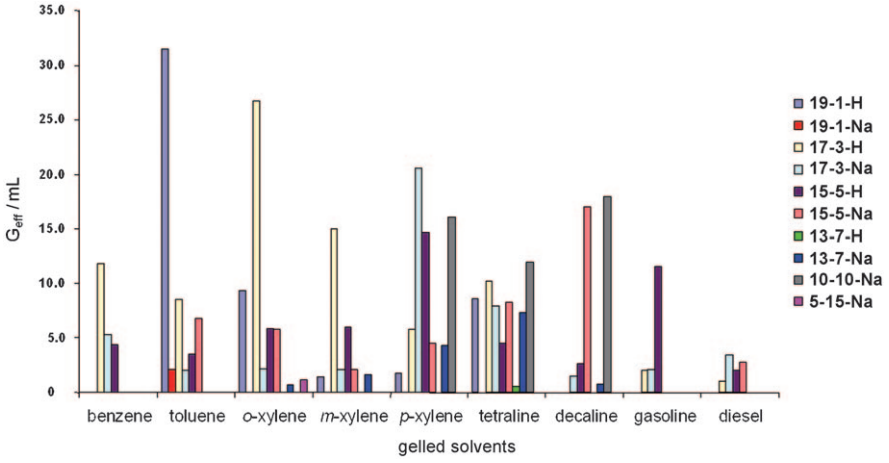

Figure 4. Comparison of gelator effectiveness (G_{eff}) values of free-acid gelators **19–1-H**, **17–3-H**, **15–5-H**, and **13–7-H** (**10–10-H** and **5–15-H** are not shown due to their lack of gelation ability) and the corresponding sodium salts **19–1-Na**, **17–3-Na**, **15–5-Na**, **13–7-Na**, **10–10-Na**, and **5–15-Na**.

Thus, transformation of the carboxylic acid end-group of **19–1-H** to the more polar sodium carboxylate of **19–1-Na** results in a dramatic decrease in the gelation effectiveness of the latter toward toluene, presumably due to its lower solubility. Comparison of the G_{eff} values for **17–3-H** (yellow bar) and **17–3-Na** (light-blue bar) shows that the former is much more efficient in the gelation of *o*- and *m*-xylenes (**17–3-H**: $G_{eff}=26.7$ and 15.0 mL; **17–3-Na**: $G_{eff}=2.2$ and 2.1 mL, respectively), while the salt gelled *p*-xylene much more efficiently (**17–3-Na**: $G_{eff}=20.6$ mL; **17–3-H**: $G_{eff}=5.8$ mL). Hence, the simple end-group transformation can in some cases dramatically change the gelator effectiveness, even toward very similar solvents such as *o*- and *p*-xylenes. Large differences in G_{eff} were also observed for **15–5-H/15–5-Na** in the gelation of *p*-xylene and decalin (Table 2, Figure 4). While **10–10-H** was found to be incapable of gelling *p*-xylene, tetralin, and decalin, **10–10-Na** exhibited very efficient gelation of these solvents, giving G_{eff} values of 16.1, 12.0, and 18.0 mL, respectively.

As in the case of some acid-type gelators, large differences in gelator effectiveness, particularly of **17–3-Na** toward *o*-, *m*-, and *p*-xylenes ($G_{eff}=2.2$, 2.1, and 20.6 mL, respectively), were observed, showing that this gelator is capable of immobilizing a tenfold larger volume of *p*- than of *o*- or *m*-xylene. The results of this gelation study show that transformation of the carboxylic acid end-group to the sodium carboxylate in these positionally isomeric gelators may generate a much more effective gelator for specific solvents (compare **17–3-Na/17–3-H** for gelling *p*-xylene; **15–5-Na/15–5-H** for gelling decalin, and **10–10-Na** efficiently gelling *p*-xylene, tetralin, and decalin in contrast to non-gelling **10–10-H**).

Optically pure versus racemic gelators in the gelation of isomeric xylenes: The influence of stereochemistry on the gelation properties of chiral gelators is very well documented.[15] In the majority of the published results, the pure enantiomer was seen to be a more effective gelator than the racemate, although several exceptions have also been reported.[14] However, symmetrical *meso* forms of various gelators have as a rule been found to lack any gelation ability.[15d,16] Since racemic **17–3-H**, **17–3-Na**, **15–5-H**, and **10–10-Na** exhibited surprisingly different G_{eff} values in the gelation of isomeric xylenes, we decided to investigate whether these properties were a consequence of their positional isomerism or a result of their stereochemical form. We prepared their optically active forms and compared the gelling properties of the enantiomers and racemates toward isomeric xylenes. The optically active free-acid and sodium salt derivatives were prepared starting from (*R*)-phenylglycine following the reaction sequences outlined in Scheme 1.

Figures 5a and b compare the G_{eff} values of *rac*- and (*R*)-free-acid and sodium salt gelators determined for isomeric xylenes and reveal dramatic differences in some cases. While *rac*-**17–3-H** showed high effectiveness in the gelations of *o*-xylene ($G_{eff}=26.7$ mL) and *m*-xylene ($G_{eff}=15.0$ mL), it was only capable of gelling a much smaller volume of *p*-xylene ($G_{eff}=5.8$ mL). In contrast, the (*R*)-enantiomer showed similarly high degrees of effectiveness toward all three isomeric xylenes (G_{eff} for *o*-, *m*-, and *p*-xylenes: 19.3, 22.2, and 19.0 mL, respectively), thus being a better gelator than the racemate for the latter two solvents (Table 3 and

Table 3. Gelation efficiencies (G_{eff}, mL) and MGC values (in parentheses; 10^{-3} mol dm^{-3}) of racemic and optically active acids and sodium salts in the gelation of isomeric xylenes.

	o-Xylene	*m*-Xylene	*p*-Xylene
17–3-H	26.7 (0.72)[b]	15.0 (1.29)[b]	5.8 (3.34)[b]
(*R*)-**17–3-H**	19.3 (1.00)[a]	22.2 (0.87)[b]	19.0 (1.02)[b]
15–5-H	5.9 (3.28)[a]	6.0 (3.22)[b]	14.7 (1.32)[b]
(*R*)-**15–5-H**	0.5 (38.7)[a]	0.8 (24.2)[a]	0.2 (96.8)[a]
10–10-H	cr.	cr.	cr.
(*R*)-**10–10-H**	0.2 (96.8)[a]	0.2 (96.8)[a]	0.6 (32.2)[a]
17–3-Na	2.2 (8.44)[b]	2.1 (8.84)[b]	20.6 (0.90)[b]
(*R*)-**17–3-Na**	1.3 (14.3)[b]	1.8 (10.3)[b]	1.2 (15.5)[a]
15–5-Na	5.8 (3.20)[b]	2.1 (8.84)[b]	4.5 (4.12)[b]
(*R*)-**15–5-Na**	5.8 (3.20)[b]	17.0 (1.09)[b]	16.8 (1.10)[b]
10–10-Na	v.s.	v.s.	16.1 (1.15)
(*R*)-**10–10**[6c]	v.s.	v.s.	1.0 (18.6)

[a] Colorless opaque gel. [b] Colorless transparent gel. Abbreviations: cr. = crystals, w. = wax-like precipitate, v.s. = viscous solution.

Figure 5a). Very large differences in G_{eff} were also found for racemic and optically active **15–5-H**; racemic **15–5-H** gelled moderate volumes of *o*-xylene ($G_{eff}=5.9$ mL) and *m*-xylene ($G_{eff}=6.0$ mL) and a large volume of *p*-xylene ($G_{eff}=14.7$ mL), while (*R*)-**15–5-H** proved to be a very poor gelator of all three solvents (G_{eff} values for *o*-, *m*-, and *p*-xylenes: 0.5, 0.8, and 0.2 mL, respectively). In the latter case, the racemate was seen to be a much more effective gelator for all three isomeric xylenes than the (*R*)-enantiomer. Indeed, considering only the gelation of *p*-xylene, the racemate exhibited a G_{eff} value more than 70 times higher than that of the (*R*)-enantiomer.

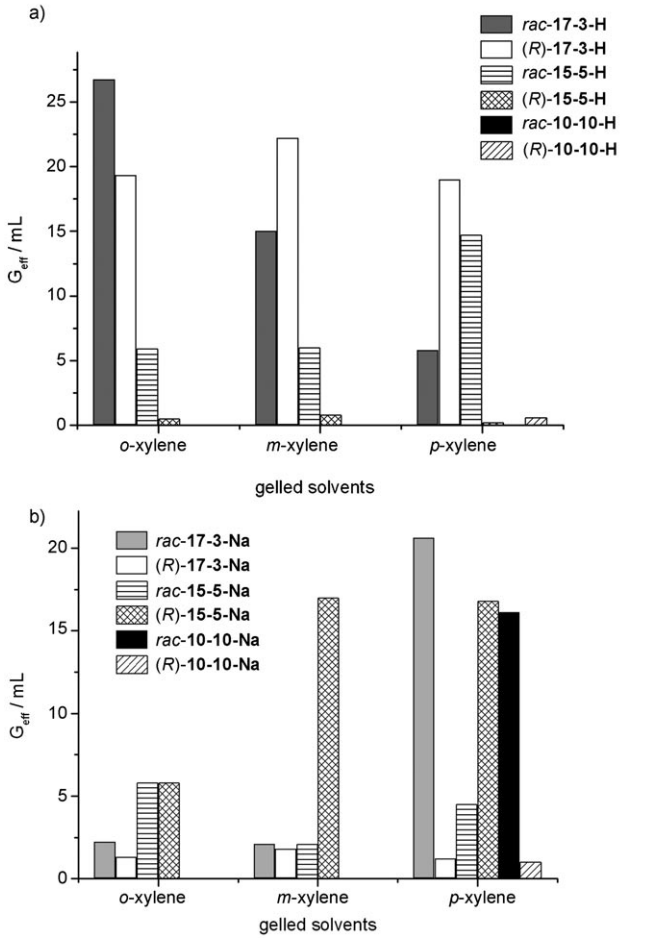

Figure 5. Gelator effectiveness G_{eff} [mL] values obtained in the gelation of xylene isomers by racemic and optically active acids a) and sodium salts b).

Comparison of the G_{eff} values of the racemic and optically active sodium salt gelators (Figure 5b) shows that *rac*-**17–3-Na** is capable of gelling an almost tenfold larger volume of *p*-xylene ($G_{eff}=20.6$ mL) than of *o*-xylene ($G_{eff}=2.2$ mL) or *m*-xylene ($G_{eff}=2.1$ mL), while the (*R*)-enantiomer showed much less efficient gelation of all three isomeric xylenes (G_{eff} values for *o*-, *m*-, and *p*-xylenes: 1.3, 1.8, and 1.2 mL, respectively). Thus, racemic **17–3-Na** was found to be a 17 times more effective gelator of *p*-xylene than its (*R*)-enantiomer. In contrast, racemic **15–5-Na** gelled only moderate volumes of isomeric xylenes (G_{eff} values for *o*-, *m*-, and *p*-xylenes: 5.8, 2.1, and 4.5 mL, respectively), while (*R*)-**15–5-Na** exhibited excellent gelation of *m*- and *p*-xylenes ($G_{eff}=17.0$ and 16.8 mL, respectively), but only gelled a moderate volume of *o*-xylene ($G_{eff}=5.8$ mL). Racemic **10–10-Na** showed excellent gelation of *p*-xylene ($G_{eff}=16.1$ mL) but gave waxy precipitates with the other two xylenes; in contrast, its (*R*)-enantiomer proved to be capable of only weak gelation of *p*-xylene ($G_{eff}=1.0$ mL). These results clearly show that the effectiveness of a gelator in the gelation of even very similar solvents can be highly dependent on its stereochemical form. Hence, in searching for highly efficient gelators for a targeted solvent, both the racemic and optically pure forms of each gelator should be prepared and tested.

As shown in Figure 3, the G_{eff} values of the racemic **19–1-H**, **17–3-H**, and **15–5-H** obtained for the gelation of isomeric xylenes are not related to their lipophilicities or the solubilities of the gelator assemblies. Hence, the most plausible explanation for the large difference in G_{eff} values observed for the enantiomer and the racemate in the gelation of the same solvent seemingly originates from different supramolecular organization of the two stereochemical forms.

In cases in which the racemate appeared to be more effective than the enantiomer (*rac*-**15–5-H**/(*R*)-**15–5-H** and *rac*-**17–3-Na**/(*R*)-**17–3-Na** *p*-xylene gels), it may have undergone spontaneous resolution into enantiomeric assemblies, which may then have interacted at a higher level of supramolecular organization giving diastereomeric assemblies.[14] In support of this interpretation, poly(D-lysine) and poly(L-lysine) were found to show a much higher propensity to form aggregated β-sheet structures in water compared to the pure enantiomers.[17] The thermodynamic driving force for such diastereoisomeric aggregation appears to be the increased water entropy gained by the diastereoisomeric packing mode. Hence, similar entropy gain can be assumed for the gelation of certain organic solvents by racemic gelators as a result of diastereoisomeric aggregation. The formation of more densely packed diastereoisomeric assemblies may result in thinner, more tightly packed gel fibers compared to those formed in the enantiomer gel. Indeed, as reported for chiral bis(amino acid)oxalamide gelators, much thinner fibers were observed by TEM in toluene gels with the racemate than with the enantiomer and the increased effectiveness of the racemate was explained in terms of the formation of a denser gel network capable of immobilizing a larger volume of toluene.[14] However, the opposite was also observed in another case, in which the racemate organized in much thicker fibers than the enantiomer.[18] Apparently, in the same solvent the racemic and optically active gelators may give gel fibers of different morphologies. As was also recently shown, racemic and pure enantiomer bola-amphiphilic gelators exhibited very similar molecular level organization in hydrogels; however, these were transformed into final assemblies of distinctly different morphologies, such as flat ribbons in the racemate gels and chirally twisted or heli-

cal ribbons in the enantiomer gels.[19] The largest differences in G_{eff} between the racemic **15–5-H** and **17–3-Na** and their enantiomeric forms (*R*)-**15–5-H** and (*R*)-**17–3-Na** were found in the gelation of *p*-xylene, the differences being less pronounced (**15–5-H**) or insignificant (**17–3-Na**) in the gelation of *o*- or *m*-xylenes. This suggests that the processes of spontaneous resolution into enantiomeric assemblies followed by diastereomeric aggregation could also be strongly influenced by the solvent structure. Recently obtained evidence for the co-organization of solvent molecules at the periphery of gelator pre-aggregates having a direct influence on the self-assembly process supports this conclusion.[3a]

^{1}H NMR and FTIR investigations: **organization at the molecular level**: In some cases, heating of gel samples for ^{1}H NMR analysis resulted in the appearance and increase of gelator signals due to gel network disassembly into smaller NMR-observable aggregates.[11,16,20] On the other hand, some gels are thermally stable in the accessible temperature range for common NMR solvents and no increase of the gelator signals could be observed upon heating of the samples. Analysis of the chemical shift changes that accompany thermally induced disassembly may give valuable information on the intermolecular interactions stabilizing the gelator aggregates and consequently on the self-assembled motifs involved.[11] The temperature dependences of the ^{1}H NMR spectra of **15–5-H** and **15–5-Na** in their gels with [D_8]toluene were investigated. For this purpose, **15–5-H** and **15–5-Na** [D_8]toluene gel samples ($c_{tot}=0.0058$ and $0.0031\,mol\,dm^{-3}$, respectively) were prepared with 1,1,2,2-tetrachloroethane (0.5 mol/mol of the gelator) as an internal standard. The concentrations of the NMR-observable gel aggregates were calculated by comparing the intensities of selected gelator signals with that of the internal standard. In the spectrum of the **15–5-H** [D_8]toluene gel acquired at room temperature, none of the gelator signals could be observed. On increasing the temperature to 35 °C, 8 % of the total gelator concentration was detected; at 45 °C, this value increased to 80 %, and at 55 °C it increased to 90–100 %, showing that at the latter temperature most of the network had been disassembled into NMR-observable aggregates. In contrast, heating of the **15–5-Na** [D_8]toluene gel sample ($c_{tot}=3.1\times10^{-3}\,mol\,dm^{-3}$) from 25 to 95 °C failed to produce any significant appearance of the gelator signals. This showed that the gel was thermally stable in the specified temperature range and that no significant disaggregation of the network into dissolved NMR-observable aggregates occurred. The temperature dependence of the chemical shifts of **15–5-H** (Figure 6) was studied at a gelator concentration in the NMR tube slightly below its experimentally determined MGC for [D_8]toluene. At $c_{tot}=5.8\times10^{-3}\,mol\,dm^{-3}$, the sample was highly viscous, indicative of the presence of highly aggregated species that were expected to be similarly organized as in the gel state. At up to 55 °C, the signals of both amide NH protons, some phenyl protons, NH-(CH_2), and the methine proton (C*H) were shifted downfield (Figure 6a); a further increase of the temperature from 55 to 95 °C caused upfield shifts of all of the signals. In this interval, large temperature coefficients ($\Delta\delta_{NH}/\Delta T$) of 13×10^{-3} and $17.8\times10^{-3}\,ppm\,K^{-1}$ were determined for -(CO)NH-(CH_2) and (C*)-NH(CO-), respectively, these being characteristic of amido NH protons engaged in hydrogen bonding. A significant upfield shift ($\Delta\delta_{C*H}/\Delta T=6\times10^{-3}\,ppm\,K^{-1}$) was also observed for the C*H proton, which is closest to the strong hydrogen bond formed by the neighboring amide group. A plausible explanation would seem to be that the C*H proton is deshielded in the aggregate by the anisotropic effect of the nearby amide carbonyl oxygen of the second molecule and hence becomes shielded upon disaggregation.

The signals of some of the methylene protons (-CH_2-CH_2-CONH- and -CH_2-CH_2-CH_3) were also slightly downfield shifted on increasing the temperature from 25 to 95 °C;

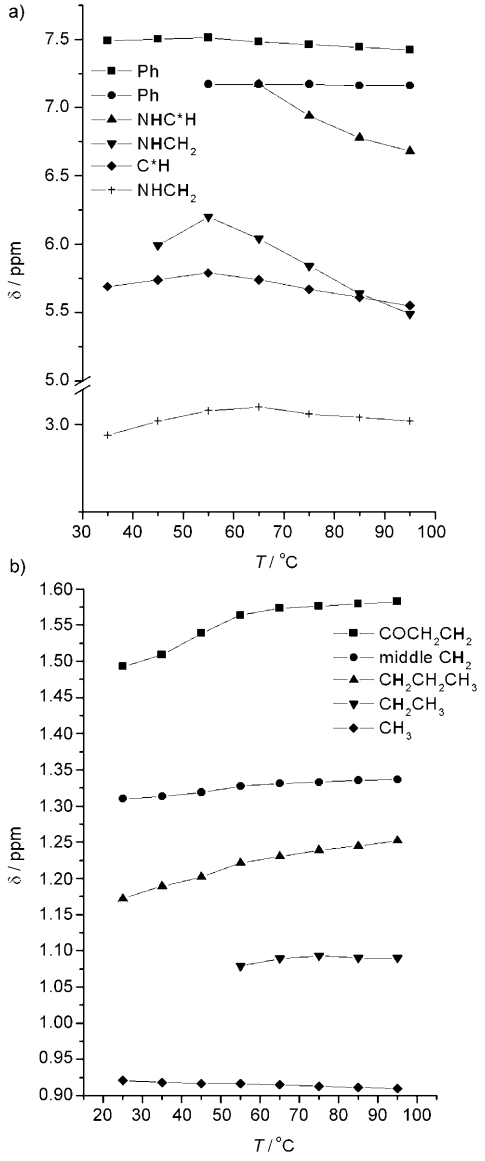

Figure 6. Temperature-induced variations in the ^{1}H NMR shifts of selected protons of **15–5-H** in [D_8]toluene.

these shifts may also be explained in terms of shielding of the relevant protons in the aggregates and their deshielding upon disaggregation. These observations indicate that the intermolecular lipophilic interactions between alkyl chains also contribute to the stabilization of the aggregates.

In the FTIR spectra of xerogels obtained by solvent removal from **17–3-Na** and **15–5-H** *o*- and *p*-xylenes (Table 4), the NH, amide I, and amide II bands appear at 3308–3299, 1637–1638, and 1532–1560 cm^{-1}, respectively, and correspond to hydrogen-bonded peptidic units.

Table 4. Selected bands [cm^{-1}] in the FTIR spectra of **17–3-Na**, **15–5-H**, and (*R*)-**15–5-H** xerogels prepared from their *o*- and *p*-xylene gels.

Xerogel/gelled solvent	ν NH	ν_{as} C–H	ν_s C–H	ν C=O; amide I	δ NH amide II	ν C=O–CO(O^-) or -CO(OH)
17–3-Na *o*-xylene	3299	2918	2849	1637	1560	1717
15–5-H *o*-xylene	3308	2915	2849	1638	1532	1719
17–3-Na *p*-xylene	3299	2918	2848	1637	1560	1715
15–5-H *p*-xylene	3308	2916	2848	1638	1533	1719
(*R*)-**15–5-H** *p*-xylene	3304	2916	2849	1637	1534	1731

The asymmetric and symmetric C–H stretching vibrations appear at low wavenumbers, 2915–2918 cm^{-1} and 2848–2849 cm^{-1}, respectively, which are characteristic of constrained alkyl chains in the aggregates[21] and are also in accord with the intermolecular alkyl chain interactions postulated on the basis of NMR data. In the case of the carboxylic acid gelator **15–5-H**, the vibration of the carboxylic acid group appears at 1719 cm^{-1}. This indicates a possible lateral type of hydrogen bonding, as found previously in some polycarboxylic acid derivatives.[22]

The ^{1}H NMR and FTIR results show that the gel aggregates of both the acid **15–5-H** and the sodium salt **17–3-Na** gelators are stabilized by cooperative hydrogen bonding between peptidic units and lipophilic interactions between alkyl chains. It should also be noted that the respective FTIR vibrations of both gelators in the spectra of their *p*-xylene and *o*-xylene gels are practically identical, despite the fact that both showed much more efficient gelation of the former solvent. The same can be concluded from comparison of the FTIR spectra of racemic **15–5-H** and (*R*)-**15–5-H** *p*-xylene gels, which differ only in the position of the carboxylic acid vibration at 1719 and 1731 cm^{-1}, respectively. The band at 1731 cm^{-1} indicates the formation of carboxylic acid dimers,[21,23] as opposed to the lateral carboxylic acid hydrogen bonding that seems to dominate in the assemblies of the racemates.

Figure 7 shows possible parallel and antiparallel β-sheet hydrogen-bonding motifs of **15–5-H**. It should be noted that the antiparallel β-sheet arrangement is less favorable compared to the parallel one due to weaker lipophilic interactions between the terminal alkyl chains. This appears to be particularly significant for **15–5-H** and **17–3-H**, which have peptidic hydrogen-bonding units closer to their carboxylic acid termini. Molecular modeling showed the **17–3-H** antiparallel dimer to be 8 kcal mol^{-1} less stable than the parallel β-sheet dimer.[24] This result, together with the fact that the amide I bands in the FTIR spectra of each of the xerogels appeared at 1637–1638 cm^{-1} (Table 4) and no band at 1695 cm^{-1} characteristic of an antiparallel β-sheet[25] could be observed, strongly suggests the formation of parallel β-sheets.

Powder XRD and TEM investigations of 17–3-Na and 15–5-H *o*- and *p*-xylene gels: Powder X-ray diffraction (PXRD) patterns obtained for xerogels of **17–3-Na** or **15–5-H** with *o*- and *p*-xylenes were seen to be very similar (Figure 8a, b). Intense peaks at $2\theta \approx 5.7$, 7.6, 9.5, 10.9, 19.5, and 22.7°, corresponding to distance periodicities *d* of 15.6, 11.6, 9.2, 8.1, 4.5, and 3.9 Å, respectively, were common to the PXRD spectra of each of the gelator molecules, implying a similar layered organization in each case.

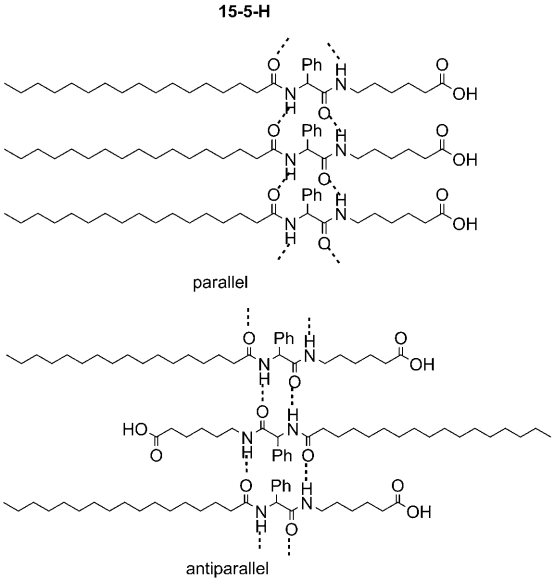

Figure 7. Intermolecular hydrogen bonding of **15–5-H** giving parallel and antiparallel β-sheet organization. ^{1}H NMR and FTIR results suggest formation of the parallel β-sheet.

It should be emphasized that despite the structural difference of **17–3-Na** and **15–5-H** and the significantly more efficient gelation of *p*-xylene than of *o*-xylene, the PXRD profiles of all four xerogels appeared very similar. The PXRD profiles of *o*- and *p*-xylene xerogels of **13–7-Na**, having a much shorter terminal chain than its positional isomer **17–3-Na**, were also determined. Again, the PXRD patterns for **13–7-Na** *o*- and *p*-xylene xerogels were found to be practically identical, with the most intense peaks corresponding to *d* spacings of 16.3, 12.2, 8.06, 4.5, and 4.08 Å. These distance

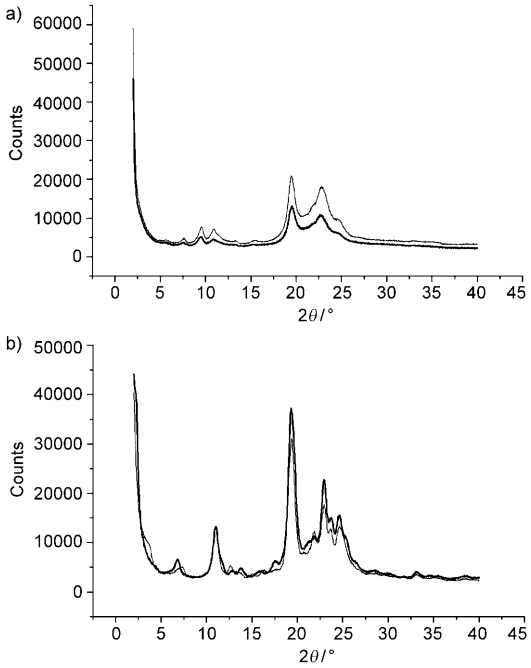

Figure 8. Powder X-ray diffraction (PXRD) patterns for a) **17–3-Na** and b) **15–5-H** xerogels prepared from *o*-xylene (thinner line) and *p*-xylene (thicker line) gels.

periodicities for the most intense peaks are close to those obtained for the **17–3-Na** and **15–5-H** xerogels. It was shown that, in contrast to **17–3-Na** and **15–5-H**, **15–5-Na** gelled similar volumes of *o*- and *p*-xylenes (Table 2); the periodic distances *d* found in the PXRD profiles of **15–5-Na** *o*- and *p*-xylene xerogels were again very similar, 12.2, 9.8, 8.1, 4.5, and 4.06 Å and 11.7, 9.2, 8.1, 4.5, and 3.97 Å, respectively, these *d* spacings being similar to those found for the **15–5-H** xerogels.

Taking into account the antiparallel β-sheet-type of molecular organization suggested by the ^{1}H NMR and FTIR investigations, a molecular modeling study was undertaken. The **17–3-H** antiparallel hydrogen-bonded dimer was generated by docking of two molecules of the gelator. A model containing two parallel stacked dimers was generated, which gave intermolecular distances of 4.5 and 4.0 Å, in accord with the periodic distances and their multiplicities found in the PXRD profiles of each of the examined xerogels (Figure 9).

The results obtained from PXRD studies of selected xerogels strongly suggest that the positionally isomeric sodium salt gelators **17–3-Na** and **15–5-Na**, as well as the free-acid gelator **15–5-H**, organize into very similar layered structures in both their *o*- and *p*-xylene gels, despite the fact that large differences in G_{eff} were observed in the gelation of these solvents. The results strongly suggest that the differences in G_{eff} are most likely a consequence of their different assemblies at a higher level of supramolecular organization, involving interactions between fibrous assemblies that ultimately give rise to fiber bundles of different dimensions and morphologies.

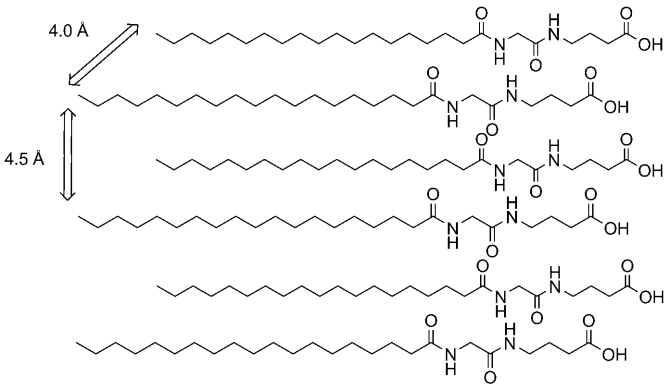

Figure 9. Possible packing of **17–3-H** parallel β-sheets proposed on the basis of ^{1}H NMR and FTIR investigations, PXRD distance periodicities in the xerogels, and molecular modeling.

The morphologies and fiber dimensions in *o*-, *m*-, and *p*-xylene gels were examined by TEM. An image of the **17–3-H** *o*-xylene gel network (Figure 10a) shows the presence of fiber bundles with diameters in the range 50–240 nm, which have a clearly visible inner structure made up of many aligned thinner fibers with diameters between 10 and 14 nm. The *m*-xylene gel (Figure 10b) comprises somewhat shorter and narrower tape-like bundles with diameters of 45–130 nm, which also consist of thinner fibers with a similar range of diameters as in the *o*-xylene gel. However, a TEM image of the *p*-xylene gel (Figure 10c) shows a distinctly different morphology characterized by the presence of relatively short bundles of pronounced tape-like shapes having widths in the range 60–90 nm. The large tapes are well structured and consist of smaller stacked tapes or fibers with diameters in the range 9–18 nm.

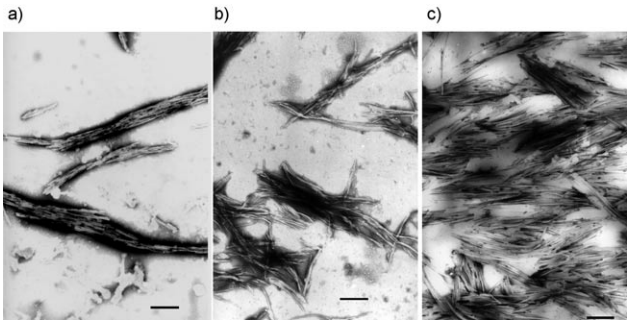

Figure 10. TEM images of **17–3-H** gels (dipotassium polytungstate (PWK)-stained; bar = 500 nm): a) *o*-xylene, b) *m*-xylene, and c) *p*-xylene.

As described above (Table 1 and Figure 2), **17–3-H** is a much more efficient gelator of *o*-xylene (G_{eff} = 26.7 mL) than of *m*-xylene (G_{eff} = 15.0 mL) or *p*-xylene (G_{eff} = 5.8 mL). TEM analyses of the *o*-, *m*-, and *p*-xylene gel morphologies showed that each gel contained thinner fibers with similar diameters in the range 10–20 nm, but that these

gave rise to different higher assemblies with a preference for tape-like aggregates in the *m*- and *p*-xylene gels.

The latter morphology could explain the observed less efficient gelation of *m*- and *p*-xylenes, since a less dense gel network with lower solvent immobilization capacity can be expected to be formed by wider and less flexible tape-like assemblies. In contrast, the TEM image of the **17–3-H** *o*-xylene gel shows the presence of large fiber bundles consisting of many tiny fibers and an absence of any tape-like assemblies. It should be emphasized, however, that the observed large dimensions of the bundles may not reflect the actual gel state and could be a consequence of the adherence of many tiny fibers during the TEM experiment.

TEM images of the **17–3-Na** *o*- and *p*-xylene gels (Figure 11a, b) show different morphologies compared to the **17–3-H** gels with the same solvents. The sodium salt gelator in *o*-xylene forms tiny flexible fibers with a rather uniform distribution of diameters in the range 16–20 nm. In the *p*-xylene gel, flexible but longer fibers with the same distribution of diameters could also be observed. Hence, compared to the **17–3-H** gels, the corresponding sodium salt shows a lower tendency for bundling and aggregation into tape-like assemblies. The fact that **17–3-Na** gelled *p*-xylene much more efficiently than *o*-xylene is again reflected in the fiber morphology, which shows the formation of longer and flexible fibers in the former gel that are capable of efficient networking. The positionally isomeric **15–5-Na** ($G_{eff}=4.5$ mL) is a much less efficient gelator of *p*-xylene than **17–3-Na** ($G_{eff}=20.6$ mL) and a TEM image (Figure 11c) showed the presence of short and thick fiber bundles (diameters 70–120 nm) in **15–5-Na** *p*-xylene gel, in sharp contrast to the presence of long and thin flexible fibers in the **17–3-Na** *p*-xylene gel.

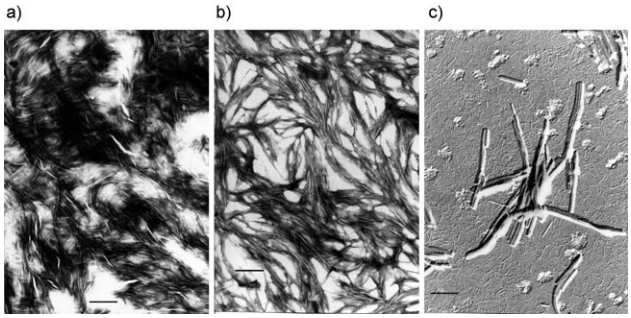

Figure 11. TEM images of **17–3-Na** gels with a) *o*-xylene and b) *p*-xylene (PWK-stained; bar = 500 nm) and c) **15–5-Na** *p*-xylene gel (Pd shadowed).

Thus, TEM investigations of the gel morphologies revealed distinct differences in the shapes and dimensions of gel fibers formed in *o*-, *m*-, and *p*-xylenes, which could be related to gelator effectiveness. By careful analysis of the TEM images, the diameters of the thinnest fibers involved in bundling could be ascertained to be in the range 10–20 nm. Taking into account the proposed model of molecular organization consisting of aggregated β-sheet chains (Figure 9), and considering the length of the gelator in the fully extended form of around 3 nm, the diameters of the finest fibers observed by TEM could be rationalized in terms of the aggregation of two to three reversed bilayers each of width around 6 nm.

Gel-to-sol transition diagrams and DSC investigation: The concentration dependences of the gel-to-sol transition temperatures (T_g) of **17–3-H** and **15–5-H** *o*-, *m*-, and *p*-xylene gels are shown in Figures 12a and b, respectively. The T_g temperatures determined by the common tube inversion method increased with increasing concentration of **17–3-H** in each of the isomeric xylene gels, reaching the same plateau T_g value of about 72 °C at 12.5 mM. Hence, the thermal stabilities of the **17–3-H** *o*-, *m*-, and *p*-xylene gels are similar, despite the fact that gelator effectiveness is much higher for *o*-xylene ($G_{eff}=26.7$ mL) than for *m*-xylene ($G_{eff}=15.0$ mL) or *p*-xylene ($G_{eff}=5.8$ mL). In contrast, at a gelator concentration of 15 mM, the T_g of the **15–5-H** *p*-xylene gel, with a gelator effectiveness (G_{eff}) of 14.7 mL, is about 7 °C higher than those of the less efficiently gelled *m*- and *o*-xylenes (G_{eff} values of 6.0 and 5.9 mL, respectively). Clearly, the positionally isomeric **17–3-H** and **15–5-H** show different thermally induced gel-to-sol transition behavior in the sense that the higher G_{eff} of **15–5-H** for *p*-xylene is also reflected in higher gel thermal stability.

The *o*- and *p*-xylene gels of the racemic **17–3-H**, **17–3-Na**, and **15–5-H** and optically active (*R*)-**17–3-Na** and (*R*)-**15–5-H** were also investigated by DSC (Figure 13a, b, and c, respectively; Table 5). In the DSC traces of the heating and cooling cycles, distinct differences between the *o*- and *p*-xylene gels could be observed. In most cases, multiple transitions were observed, indicating the polymorphic character of the present assemblies. In the heating cycles of the **17–3-H** *o*- and *p*-xylene gels, enthalpy changes of 20.93 and 39.94 kJ mol^{-1}, respectively, were measured for the first transitions, $T_{m1}=78.6$ and 77.8 °C, which correspond to the T_g temperatures determined independently by tube inversion. The difference between the first transition ΔH_m values for the *o*- and *p*-xylene gels amounted to 19 kJ mol^{-1}, suggesting different organization of the assemblies formed in the *o*- and *p*-xylene gels. In contrast, for the **17–3-Na** *o*- and *p*-xylene gels, different DSC characteristics were observed. The measured ΔH_m difference of only 3 kJ mol^{-1} between the first transitions in the **17–3-Na** *o*- and *p*-xylene gels is much smaller than that obtained for the **17–3-H** gels.

Here, the predominant formation of assemblies of similar structure and thermal stability could be postulated in both gels. In the **17–3-H** *p*-xylene gel, the presence of two additional polymorphic assemblies with small contributions to the total ΔH_m could be observed (Figure 13a and Table 5). However, for the **17–3-Na** *p*-xylene gel, a significant ΔH_m contribution of 28.33 kJ mol^{-1} from the second transition and a minor contribution of 2.02 kJ mol^{-1} from the third transition were observed, which were absent from the DSC trace of the *o*-xylene gel. In the latter case, significant for-

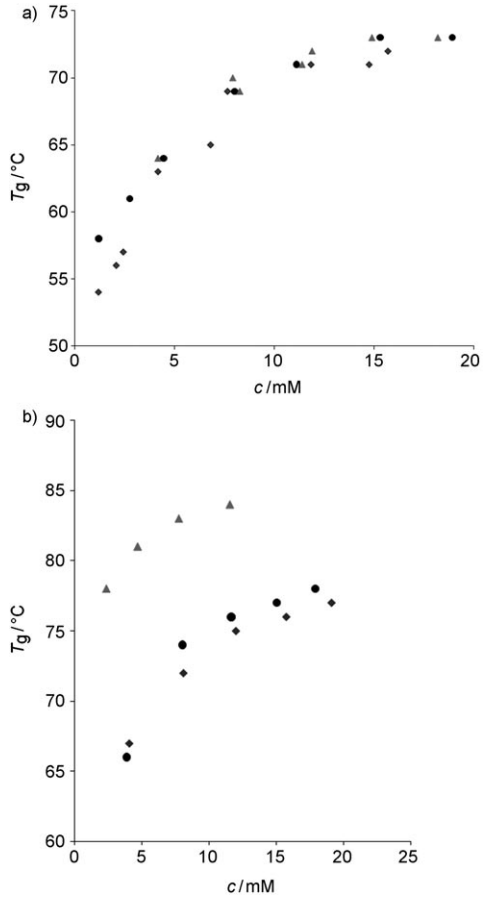

Figure 12. Gel-to-sol transition diagrams of **17–3-H** a) and **15–5-H**, b) *o*-(♦), *m*- (●), and *p*-(▲)-xylene gels.

mation of polymorphic assemblies in the *p*-xylene gel may contribute to more efficient networking, thereby resulting in the formation of a denser network with higher solvent immobilization capacity compared to that formed in the *o*-xylene gel. This offers a likely explanation for the much higher G_{eff} of **17–3-Na** toward *p*-xylene compared to that for *o*-xylene, with which such polymorphic assemblies are absent. The DSC results for the **15–5-H** *o*- and *p*-xylene gels resemble those obtained for the **17–3-H** gels, although for the first transitions in the **15–5-H** *o*- and *p*-xylene gels an even larger ΔH_m difference of 31 kJ mol^{-1} was measured (Table 5). While for the **15–5-H** *p*-xylene gel three different polymorphs could be observed, DSC showed only one transition for the corresponding *o*-xylene gel, indicating the presence of only one type of assembly. It should be noted that the enthalpy changes for the first transitions measured for the (*R*)-**15–5-H** *o*- and *p*-xylene gels ($\Delta H_m = 41.91$ and 52.19 kJ mol^{-1}, respectively) are much closer to that for the racemic **15–5-H** *o*-xylene gel ($\Delta H_m = 55.73$ kJ mol^{-1}) than to that for the *p*-xylene gel ($\Delta H_m = 87.19$ kJ mol^{-1}).

The DSC investigations allowed deeper insight into the rather complex organization of the racemic gelators in their *o*- and *p*-xylene gels. The results showed that with the racemic gelators and very similar solvents, different numbers of polymorphic assemblies of different energy could be formed. It should be noted that for all three racemic gelators, **17–3-H**, **17–3-Na**, and **15–5-H**, three different polymorphs could be observed in their *p*-xylene gels (Table 5), as compared to two or only one in *o*-xylene. Moreover, in contrast to the three polymorphs observed in the racemic **15–5-H** *p*-xylene gel, its optically active form gave only a single polymorph in its *p*-xylene and *o*-xylene gels. Hence, the racemic gelators showed a higher tendency to self-assemble into polymorphic assemblies than the optically pure gelators, and this tendency was clearly stronger for *p*- than for *o*-xylene. The presented results strongly bring into focus the role of solvent in the gelation process. It can be concluded that both in the case of spontaneous resolution and in the formation of different polymorphs, specific solvation effects have a high impact on the observed self-assembly process, even for very similar solvents such as *o*- and *p*-xylenes.

Enantiomer and racemate polymorphic assemblies: Taking into account the similar molecular level organization of gelator molecules in *o*- and *p*-xylene gels, the formation of polymorphic assemblies differing in energy could be rationalized by considering the chirality and directionality of the primary bilayer-type assemblies interacting at a higher level of supramolecular organization.

As shown schematically in Figure 14*i*), a gelator of (*R*)-configuration may organize into head-to-head bilayers with the same or opposite intermolecular hydrogen-bonding directionality; in principle, for the interacting bilayers four different polymorphs differing in hydrogen-bonding directionality could be constructed (Figure 14*ii*). In the case of a racemic gelator, a larger number of polymorphic assemblies could be constructed considering the possible formation of *meso*-bilayers built from (*R*)- and (*S*)-gelator molecules (Figure 15a, *i* and *ii*) or considering interac-

Table 5. Total enthalpy changes[a] and transition temperatures in heating (ΔH_m, kJ mol^{-1}; T_m, °C) and cooling (T_c, °C) cycles obtained by DSC measurements of **17–3-H**, **17–3-Na**, and (*R*)-**17–3-Na** *o*- and *p*-xylene gels at a concentration of each gelator of 20 mM.

	ΔH_m (T_{m1})	ΔH_m (T_{m2})	ΔH_m (T_{m3})	ΔH_m total	T_{c1}	T_{c2}	T_{c3}
17–3-H *p*-xylene	20.93 (78.6)	7.11 (105.3)	2.8 (116.3)	30.85	37.6	78.7	112.2
17–3-H *o*-xylene	39.94 (77.8)	–	8.38 (114.4)	48.32	41.6	–	–
17–3-Na *p*-xylene	43.60 (75.2)	28.33 (97.9)	2.02 (106.2)	73.96	38.4	68.4	104.5
17–3-Na *o*-xylene	40.59 (73.3)	–	–	40.59	36.8	–	–
(*R*)-**17–3-Na** *p*-xylene	28.35 (78.5)	5.8 (103.0)	–	34.18	38.6	79.8	–
(*R*)-**17–3-Na**/*o*-xylene	34.06 (74.6)	–	4.40 (113.7)	38.47	41.7	–	–
15–5-H *p*-xylene	87.19 (86.6)	1.37 (92.1)	15.67 (111.6)	104.23	27.9	42.9	109.6
15–5-H *o*-xylene	55.73 (64.9)	–	–	55.73	21.7	–	–
(*R*)-**15–5-H** *p*-xylene	52.19 (59.8)	–	–	52.19	21.3	–	–
(*R*)-**15–5-H** *o*-xylene	41.91 (53.1)	–	–	41.91	7.9	–	–

[a] "ΔH_m total" represents the sum of enthalpies for all transitions observed in the heating cycle.

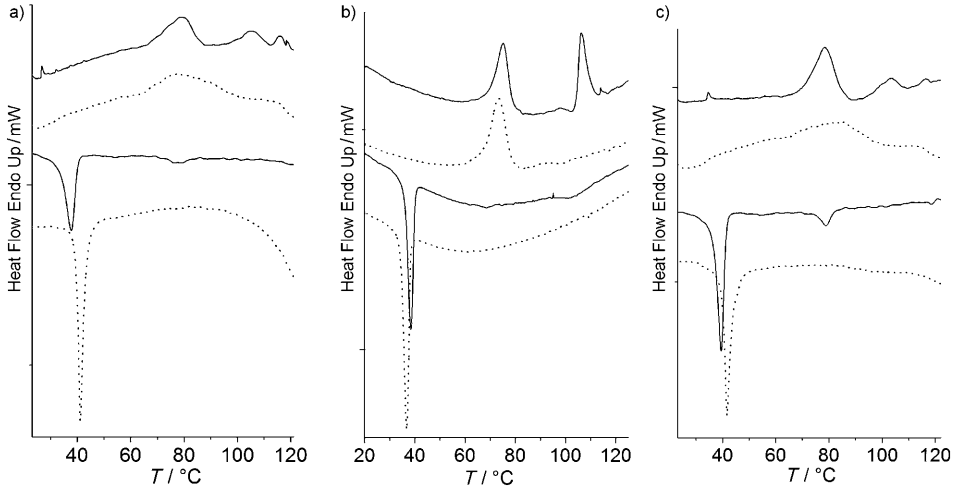

Figure 13. DSC diagrams showing heating (upper curves) and cooling (lower curves) cycles of a) **17–3-H**, b) **17–3-Na**, and c) (*R*)-**17–3-Na** *p*-xylene (solid line) and *o*-xylene (dotted line) gels.

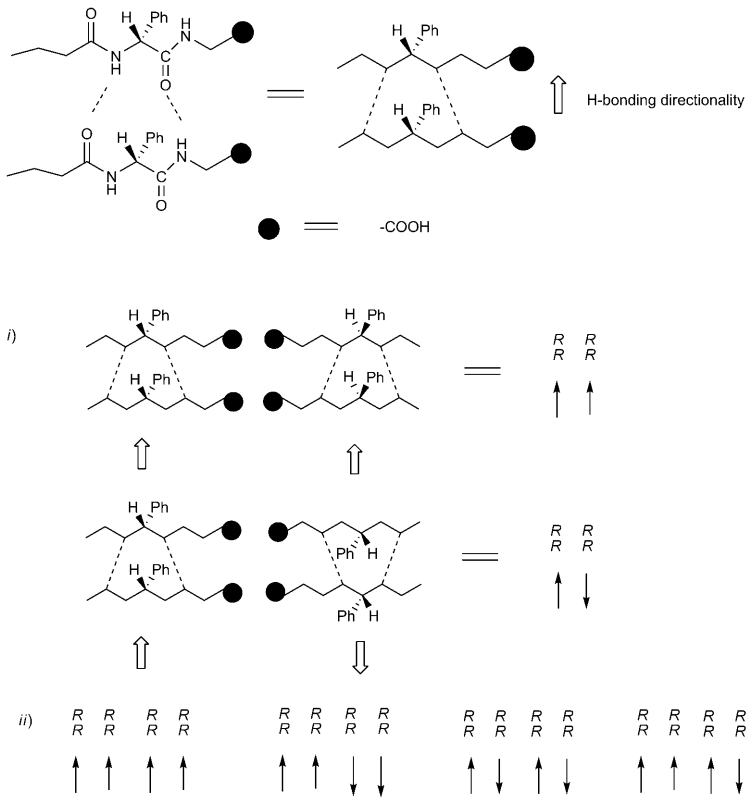

Figure 14. Schematic representation of single enantiomer interacting bilayers differing in directionality of intermolecular hydrogen bonding.

tions between enantiomeric bilayers each consisting of a single enantiomer (Figure 15b, i and ii). In the first case of the *meso*-bilayer, three polymorphs with intra- and inter-bilayer symmetry and one lacking inter-bilayer symmetry may be postulated. The formation of such highly symmetric assemblies is favorable for crystallization, as predicted by Fuhrhop's "chiral bilayer effect" formulated for amphiphilic gelators.[15i,26] In the case of interacting enantiomeric bilayers, five different polymorphs could be constructed, each lacking intra-bilayer symmetry, three of them possessing inter-bilayer symmetry, and one lacking both intra- and inter-bilayer symmetry (Figure 15b, ii). One might speculate that the formation of diastereoisomeric assemblies from interacting enantiomeric bilayers in such a way that they conserve the inter-bilayer symmetry is favorable for packing, and that this should result in the formation of thinner fibers that are capable of forming denser networks with higher solvent immobilization capacities.

Conclusion

A series of chiral, positionally isomeric gelators has been prepared by variation of the terminal and carboxylic acid alkyl chain lengths defined by descriptors *m* and *n*, respectively (Figure 1). Their gelation properties (Tables 1–3 and Figures 2–5) have been analyzed in terms of gelator versatility (G_{ver}) and gelator effectiveness (G_{eff}). The results of extensive gelation studies have shown that simple synthetic optimization of a "lead gelator molecule" by variation of the lengths of its alkyl chains, end-group polarity (carboxylic acid versus sodium carboxylate), and stereochemical form (racemate versus optically pure form) can have a tremendous influence on the G_{ver} and G_{eff} values. The results have also shown that despite the identical lipophilic/hydrophilic balance common to all of the positionally isomeric gelators, a different arrangement of the apolar (alkyl chains) and polar (peptidic and carboxylic acid) moieties within the gelator molecule is highly important and has a strong impact on their gelation properties. The positional isomerism has been found to have

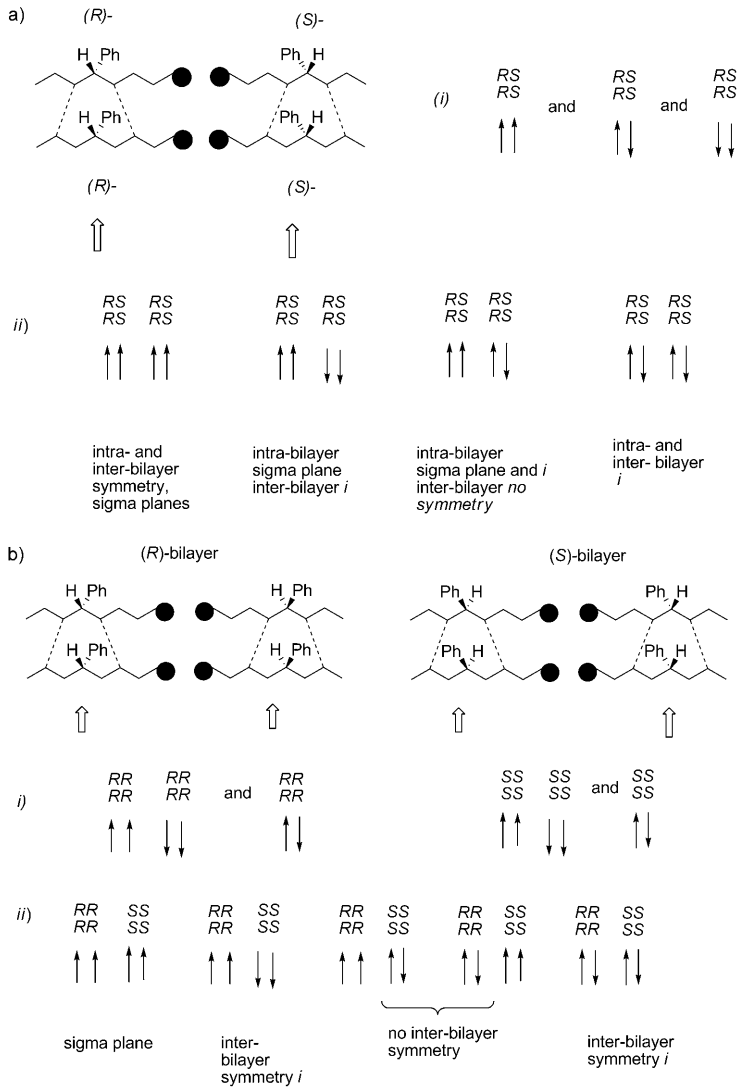

Figure 15. Schematic representation of a) *meso*-bilayers (*i*) and possible polymorphs (*ii*) and b) enantiomeric bilayers (*i*) and the polymorphs (*ii*) with intra- and inter-bilayer symmetry.

an impact on the relative lipophilicity of the isomers, as reflected in different calculated average log*P* values; they decrease with decreasing length (m) of the terminal alkyl chains and increasing length (n) of the carboxylic acid alkyl chains, making **19–1-H** the most lipophilic and **5–15-H** the least lipophilic in the series. Considering gelator versatility, of the series of racemic positionally isomeric free-acid gelators, **17–3-H** and **15–5-H** were found to be the most versatile, being capable of gelling ten of the twenty solvents tested ($G_{ver}=9$ and 10), including two highly lipophilic hydrocarbon fuels (gasoline and diesel fuel) (Table 1 and Figure 2). The most lipophilic isomer, **19–1-H**, having the longest terminal alkyl chain ($m=19$) and the shortest carboxylic acid chain ($n=1$), proved to be much less versatile than **17–3-H** and **15–5-H**, giving a G_{ver} value of only 5, while the isomers with m smaller than 15 and larger n such as **13–7-H** ($G_{ver}=1$, only slight gelation of tetralin), **10–10-H**, and **5–15-H** were practically incapable of gelling any of the tested solvents.

Modification of the gelator end-group polarity by transformation of the carboxylic acid into a sodium carboxylate group resulted in the gelation of a similar set of lipophilic aromatic solvents as gelled by the free-acid-type gelators. It thus appears that this end-group modification has limited impact on gelator versatility, making the sodium salt gelators with $m=17$, 15 and $n=3$, 5 methylene units in their alkyl chains the most versatile, as in the case of the free-acid gelators (Table 2 and Figure 3).

Much more pronounced effects of positional isomerism and end-group modification were observed with respect to gelator effectiveness (G_{eff}). For example, **19–1-H** was by far the best gelator of toluene ($G_{eff}=31.5$ mL) compared to the other positional isomers (Table 1); however, **17–3-H** proved to be superior in the gelation of *o*- and *m*-xylenes, while **15–5-H** was seen to be the most effective in the gelation of *p*-xylene (Table 1, Figures 2 and 4). Some of the free-acid-type racemic positional isomers showed up to tenfold more efficient gelation of specific solvents than other isomers. Unexpectedly, such efficiency differences appeared even in the gelation of very similar solvents such as isomeric xylenes. Evidence has been obtained (Figure 3) that, in contrast to some other types of toluene gelators, the effectiveness of the tested positional isomers cannot be correlated with the solubility of their assemblies in the gelled solvents.[5a]

Large differences in G_{eff} were also found for the positionally isomeric sodium salt gelators (Table 2, Figure 3). While **17–3-H** proved to be the most efficient gelator of *o*-xylene (G_{eff} values for *o*-, *m*-, and *p*-xylenes: 26.7, 15.0, and 5.8 mL, respectively), its Na salt (**17–3-Na**) showed the most efficient gelation of *p*-xylene (G_{eff} values for: *p*-, *m*-, and *o*-xylenes: 20.6, 2.1, and 2.2 mL, respectively). These results show that for some of the positional isomers, a simple transformation of the carboxylic acid group into the corresponding sodium carboxylate may result in a dramatic change in G_{eff} toward the same solvent (compare also the G_{eff} values for **19–1-H**/**19–1-Na** toluene gels, **17–3-H**/**17–3-Na** *m*-xylene gels, **15–5-H**/**15–5-Na** decalin gels, and **10–10-H**/**10–10-Na** *p*-xylene, tetralin, and decalin gels).

Comparison of the efficacies of the racemic and optically pure gelators in the gelation of isomeric xylenes showed in some cases large or very large differences in G_{eff} values toward the same solvent (Table 3). For example, (*R*)-**17–3-H** and its racemate displayed G_{eff} values of 19.0 and 5.8 mL, respectively, in the gelation of *p*-xylene. In contrast, the racemic **15–5-H** was found to be about 70 times more efficient in the gelation of *p*-xylene than its pure enantiomer (*R*)-**15–5-H** (G_{eff} values of 14.7 and 0.2 mL, respectively); this result represents the largest difference in G_{eff} found in this study. Large differences in G_{eff} were also found for (*R*)-**15–5-Na**/**15–5-Na** (G_{eff} ratios 8.0 and 3.7 for *m*- and *p*-xylene gels) and *rac*-**17–3-Na**/(*R*)-**17–3-Na** (G_{eff} ratio 17.1 for *p*-xylene gels). These results clearly demonstrate that the effectiveness of a gelator in the gelation of certain solvents is highly dependent on its stereochemical form. In some cases, the

racemic gelator was found to be much more efficient than the pure enantiomer, which indicates their different organization in the final gel fiber assemblies.

The results of ^{1}H NMR, FTIR, and PXRD studies revealed similar organization of the positionally isomeric gelators at the molecular level, characterized by the formation of stacked parallel β-sheet assemblies (Figures 7 and 9). TEM investigations revealed the formation of fiber bundles composed of fine fibers with diameters in the range 10–20 nm. The observed fiber dimensions suggested possible aggregation of two to three reversed bilayers each containing two extended gelator molecules of length 3 nm. The TEM images also showed clear morphology differences between the **17–3-H** and **17–3-Na** *o*- and *p*-xylene gels, the first solvent being much more efficiently gelled by **17–3-H** and the second by **17–3-Na** (Figures 10 and 11). Previous investigations have shown that thin and flexible fibers are capable of forming denser gel networks containing smaller compartments, which are capable of immobilizing larger volumes of solvent than networks built from thicker and more rigid fibers.[14,18]

DSC investigations of **17–3-H**, **17–3-Na**, **15–5-H**, and optically pure (*R*)-**17–3-Na** and (*R*)-**15–5-H** gels allowed deeper insight into the rather complex organizations coexisting in their *o*- and *p*-xylene gels. Distinct differences in the DSC traces for the *o*- and *p*-xylene gels were observed, as manifested in the number of observed transitions in both the heating and cooling cycles, as well as in the measured enthalpy changes (Table 5 and Figure 13). The large difference between the first transition enthalpy changes (ΔH_m) measured for the *o*-xylene and *p*-xylene gels of racemic **15–5-H** shows that the polymorphic assemblies formed in two similar solvents can be significantly different in energy.

Using hydrogen-bonding directionality and symmetry arguments for the racemate gels, four possible head-to-head *meso*-polymorphs could be constructed, three of them having intra- and inter-bilayer symmetry (Figure 15a). Such highly symmetrical organizations are favorable for crystallization, in accord with the chiral bilayer effect.[15i,26] In the case of spontaneous resolution followed by interactions between enantiomeric bilayers, five different polymorphs could be constructed (Figure 15b), three of them having inter-bilayer symmetry. It can be assumed that diastereomeric interactions with conserved inter-bilayer symmetry are energetically favored and lead to the formation of thinner fibers capable of efficient networking. Such fibers are capable of forming denser gel networks with higher solvent immobilization capacity, which is in turn reflected in high gelator effectiveness (G_{eff}) values. It seems that the formation of polymorphic assemblies is more pronounced in *p*-xylene than in *o*-xylene; the racemic **17–3-H**, **17–3-Na**, and **15–5-H** gave rise to three polymorphs in *p*-xylene gels, while in the *o*-xylene gels two or only one polymorph could be observed (Table 5). The presented results, together with other most recent work,[3a,5a] strongly bring into focus the role of the solvent in the gelation process, which has largely been neglected in the majority of work related to gelation. The results show that, even for very similar solvents such as isomeric xylenes, specific solvation effects may result in spontaneous resolution into enantiomeric assemblies, which is then followed by different diastereomeric aggregation leading to the formation of polymorphic assemblies. Hence, these specific solvation effects have a high impact on the self-assembly process, determining both the morphology and stability of gel fibers and consequently the solvent immobilization capacity of the network. This is reflected in sometimes dramatically different gelator effectiveness values G_{eff}, as seen, for example, for racemic **15–5-H** and its (*R*)-enantiomer, the former being a 70 times more effective gelator of *p*-xylene than the latter.

Experimental Section

All synthetic procedures, equipment used, and characterizations of the prepared compounds are summarized in the Supporting Information.

Determination of gelling properties: A sample (10 mg) of the tested substance was placed in a test tube and the requisite solvent was added by means of a microsyringe in 100–500 μL portions. After each addition, the mixture was gently heated until the substance dissolved, then allowed to cool naturally to room temperature. The formation of a gel was checked by inversion of the test tube. The procedure was repeated until sample fluidity was restored at room temperature.

Acknowledgements

Financial support from the Croatian Ministry of Science, Education, and Sport (Project 098-0982904-2912) is gratefully acknowledged. We are grateful to Dr. N. Ljubešić and L. Horvat for acquiring the TEM images and to Dr. D. Lyons and Dr. D. Medaković for performing the PXRD measurements.

[1] a) P. Terech, R. G. Weiss (Eds.), *Molecular Gels*, Springer, Dordrecht, **2006**; b) D. K. Smith, *Molecular Gels — Nanostructured Soft Materials in Organic Nanostructures* (Eds.: J. W. Steed, J. L. Atwood), Wiley-VCH, Weinheim, **2008**; c) F. Fages, *Top. Curr. Chem.* **2005**, *256*, 1–273; d) P. Terech, R. G. Weiss, *Chem. Rev.* **1997**, *97*, 3133–3159; e) J. H. van Esch, B. L. Feringa, *Angew. Chem.* **2000**, *112*, 2351–2354; *Angew. Chem. Int. Ed.* **2000**, *39*, 2263–2266; f) M. de Loos, B. L. Feringa, J. H. van Esch, *Eur. J. Org. Chem.* **2005**, 3615–3631; g) L. A. Estroff, A. D. Hamilton, *Chem. Rev.* **2004**, *104*, 1201–1217.

[2] a) R. G. Ellis-Behnke, Y.-X. Liang, S.-W. You, D. K. C. Tay, S. Zhang, K.-F. So, G. E. Schneider, *Proc. Natl. Acad. Sci. USA* **2006**, *103*, 5054–5059; b) G. A. Silva, C. Czeisler, K. L. Niece, E. Beniash, D. A. Harrington, J. A. Kessler, S. I. Stupp, *Science* **2004**, *303*, 1352–1355; c) Z. Liang, G. Yang, M. Ma, A. S. Abbah, W. W. Lu, B. Xu, *Chem. Commun.* **2007**, 843–845; d) K. J. C. van Bommel, A. Friggeri, S. Shinkai, *Angew. Chem.* **2003**, *115*, 1010–1030; *Angew. Chem. Int. Ed.* **2003**, *42*, 980–999; e) K. Sada, M. Takeuchi, N. Fujita, M. Numata, S. Shinkai, *Chem. Soc. Rev.* **2007**, *36*, 415–435; f) T. Fukushima, K. Asaka, A. Kosaka, T. Aida, *Angew. Chem.* **2005**, *117*, 2462–2465; *Angew. Chem. Int. Ed.* **2005**, *44*, 2410–2413; g) J. Puigmarti-Luis, V. Laukhin, A. Perez del Pino, J. Vidal-Gancedo, C. Rovira, E. Laukhina, D. B. Amabilino, *Angew. Chem.* **2007**, *119*, 242–245; *Angew. Chem. Int. Ed.* **2007**, *46*, 238–241; h) P. K. Vemula, G. John, *Chem. Commun.* **2006**, 2218–2220; i) Z. Yang, B. Xu, *Chem. Commun.* **2004**, 2424–2425; j) J. C. Tiller, *Angew. Chem.* **2003**, *115*, 3180–3183; *Angew. Chem. Int. Ed.* **2003**, *42*, 3072–3075;

k) S. V. Vinogradov, T. K. Bronich, A. V. Kabanov, *Adv. Drug Delivery Rev.* **2002**, *54*, 135–147.
[3] a) P. Jonkheijm, P. van der Schoot, A. P. H. J. Schenning, E. W. Meijer, *Science* **2006**, *313*, 80–83; b) D. K. Smith, *Chem. Soc. Rev.* **2009**, *38*, 684–694; c) M. de Loos, J. H. van Esch, R. M. Kellogg, B. L. Feringa, *Tetrahedron* **2007**, *63*, 7285–7301.
[4] J. H. van Esch, *Langmuir* **2009**, *25*, 8392–8394.
[5] a) A. R. Hirst, I. A. Coates, T. R. Boucheteau, J. F. Miravet, B. Escuder, V. Castelletto, I. W. Hamley, D. K. Smith, *J. Am. Chem. Soc.* **2008**, *130*, 9113–9121; b) Y. Jeong, K. Hanabusa, H. Masunga, I. Akiba, K. Miyoshi, S. Sakurai, K. Sakurai, *Langmuir* **2005**, *21*, 586–594.
[6] a) A. D′Aléo, J.-L. Pozzo, K. Heuzé, F. Vögtle, F. Fages, *Tetrahedron* **2007**, *63*, 7482–7488; b) A. D′Aléo, J.-L. Pozzo, F. Fages, M. Schmutz, G. Mieden-Gundert, F. Vögtle, V. Čaplar, M. Žinić, *Chem. Commun.* **2004**, 190–191; c) V. Čaplar, M. Žinić, J.-L. Pozzo, F. Fages, G. Mieden-Gundert, F. Vögtle, *Eur. J. Org. Chem.* **2004**, 4048–4059; d) G. Mieden-Gundert, L. Klein, M. Fischer, F. Vögtle, K. Heuzé, J.-L. Pozzo, M. Vallier, F. Fages, *Angew. Chem.* **2001**, *113*, 3266–3267; *Angew. Chem. Int. Ed.* **2001**, *40*, 3164–3166.
[7] http://www.vcclab.org/lab/alogps/.
[8] N. Zweep, A. Hopkinson, A. Meetsma, W. R. Browne, B. L. Feringa, J. H. van Esch, *Langmuir* **2009**, *25*, 8802–8809.
[9] a) V. Percec, G. Ungar, M. Peterca, *Science* **2006**, *313*, 55–56; b) X. Huang, P. Terech, S. R. Raghavan, R. G. Weiss, *J. Am. Chem. Soc.* **2005**, *127*, 4336–4344; c) A. Aggeli, I. A. Nyrkova, M. Bell, R. Harding, L. Carrick, T. C. B. McLeish, A. N. Semenov, N. Boden, *Proc. Natl. Acad. Sci. USA* **2001**, *98*, 11857–11862; d) M. de Loos, J. van Esch, R. M. Kellogg, B. L. Feringa, *Angew. Chem.* **2001**, *113*, 633–636; *Angew. Chem. Int. Ed.* **2001**, *40*, 613–616; e) A. Arnaud, L. Bouteiller, *Langmuir* **2004**, *20*, 6858–6863; f) V. Simic, L. Bouteiller, M. Jalabert, *J. Am. Chem. Soc.* **2003**, *125*, 13148–13154; g) L. Bouteiller, O. Colombani, F. Lortie, P. Terech, *J. Am. Chem. Soc.* **2005**, *127*, 8893–8898; h) J. E. A. Webb, M. J. Crossley, P. Turner, P. Thordarson, *J. Am. Chem. Soc.* **2007**, *129*, 7155–7162.
[10] a) A. Kentsis, K. L. B. Borden, *Curr. Protein Pept. Sci.* **2004**, *5*, 125–134; b) R. B. Martin, *Chem. Rev.* **1996**, *96*, 3043–3064; c) D. H. Zhao, J. S. Moore, *Org. Biomol. Chem.* **2003**, *1*, 3471–3491.
[11] J. Makarević, M. Jokić, B. Perić, V. Tomišić, B. Kojić-Prodić, M. Žinić, *Chem. Eur. J.* **2001**, *7*, 3328–3341.
[12] Such a relationship holds for the gelators studied in ref. [5a]. The average $\log P$ values calculated for these gelators and their experimentally determined MGC values (mM) and gelator assembly solubilities (c_{diss}) at 30 °C in toluene were as follows: 4-Boc, average $\log P$ 8.28, MGC 25 mM, c_{diss} = 31 mM; 2ɛZ, average $\log P$ 7.63, MGC 10 mM, c_{diss} = 3 mM; 2αZ, average $\log P$ 7.63, MGC 3 mM, c_{diss} = 0.3 mM, and 4z, average $\log P$ 6.84, MGC 3 mM, c_{diss} = 0.007 mM. Hence, the most lipophilic 4-Boc had the highest MGC and c_{diss} and exhibited the lowest effectiveness in the gelation of toluene, while the least lipophilic 4z had a low MGC and the lowest c_{diss} and proved to be the most effective gelator of toluene.
[13] a) M. Lescanne, A. Colin, O. Mondain-Monval, F. Fages, J.-L. Pozzo, *Langmuir* **2003**, *19*, 2013–2020; b) M. Lescanne, P. Grondin, A. d′Aléo, F. Fages, J.-L. Pozzo, O. Mondain-Monval, P. Reinheimer, A. Colin, *Langmuir* **2004**, *20*, 3032–3041.
[14] a) J. Makarević, M. Jokić, Z. Raza, Z. Štefanić, B. Kojić-Prodić, M. Žinić, *Chem. Eur. J.* **2003**, *9*, 5567–5580; b) A. R. Hirst, D. K. Smith, M. C. Feiters, H. P. M. Geurts, A. C. Wright, *J. Am. Chem. Soc.* **2003**, *125*, 9010–9011; c) A. R. Hirst, D. K. Smith, M. C. Feiters, H. P. M. Geurts, *Chem. Eur. J.* **2004**, *10*, 5901–5910.
[15] a) D. K. Smith, *Chem. Soc. Rev.* **2009**, *38*, 684–694; b) A. Brizard, R. Oda, I. Huc, *Top. Curr. Chem.* **2005**, *256*, 167–218; c) M. Jokić, J. Makarević, M. Žinić, *J. Chem. Soc. Chem. Commun.* **1995**, 1723–1724; d) R. Oda, I. Huc, *Angew. Chem.* **1998**, *110*, 2835–2838; *Angew. Chem. Int. Ed.* **1998**, *37*, 2689–2691; e) X. Luo, B. Liu, Y. Liang, *Chem. Commun.* **2001**, 1556–1557; f) K. Hanabusa, H. Kobayashi, M. Suzuki, M. Kimura, H. Shirai, *Colloid Polym. Sci.* **1998**, *276*, 252–259; g) K. Hanabusa, K. Okui, K. Karaki, M. Kimura, H. Shirai, *J. Colloid Interface Sci.* **1997**, *195*, 86–93; h) S. Bhattacharya, S. N. Ghanashyam Acharya, A. R. Raju, *Chem. Commun.* **1996**, 2101–2102; i) J.-H. Fuhrhop, P. Schneider, J. Rosenberg, E. Boekema, *J. Am. Chem. Soc.* **1987**, *109*, 3387–3390.
[16] M. Jokić, V. Čaplar, T. Portada, J. Makarević, N. Šijaković-Vujičić, M. Žinić, *Tetrahedron Lett.* **2008**, *50*, 509–511.
[17] W. Dzwolak, R. Ravindra, C. Nicolini, R. Jansen, R. Winter, *J. Am. Chem. Soc.* **2004**, *126*, 3762–3768.
[18] TEM investigations of some oxalamide gels have revealed that in the gel samples of the more effective gelators thinner and more flexible fibers could be observed, while with the less effective gelators thicker straight fibers were present.[11,14] It was concluded that thinner and more flexible fibers are capable of forming denser networks having smaller compartments compared to the networks formed by thicker straight fibers; since solvent is immobilized mostly by capillary forces, the former networks should possess higher solvent immobilization capacity than the latter. In this way, the morphology of the gel fibers may also affect the volume of gelled solvent.
[19] R. Oda, F. Artzner, M. Laguerre, I. Huc, *J. Am. Chem. Soc.* **2008**, *130*, 14705–14712.
[20] a) F. Menger, Y. Yamasaki, K. K. Catlin, T. Nishimi, *Angew. Chem.* **1995**, *107*, 616–618; *Angew. Chem. Int. Ed. Engl.* **1995**, *34*, 585–586; b) D. C. Duncan, D. G. Whitten, *Langmuir* **2000**, *16*, 6445–6452; c) B. Escuder, M. Llusar, J. F. Miravet, *J. Org. Chem.* **2006**, *71*, 7747–7752.
[21] M. Suzuki, T. Sato, A. Kurose, H. Shirai, K. Hanabusa, *Tetrahedron Lett.* **2005**, *46*, 2741–2745.
[22] a) J. Dong, Y. Ozaki, K. Nakashima, *Macromolecules* **1997**, *30*, 1111–1117; b) L. Sun, L. J. Kepley, R. M. Crooks, *Langmuir* **1992**, *8*, 2101–2103.
[23] A. Pal, Y. K. Ghosh, S. Bhattacharya, *Tetrahedron* **2007**, *63*, 7334–7348.
[24] SYBYL molecular modeling software of TRIPOS Inc., 1699 South Hanley Road, St. Louis, http://www.tripos.com/.
[25] S. Iqbal, J. F. Miravet, B. Escuder, *Eur. J. Org. Chem.* **2008**, 4580–4590.
[26] P. Terech, V. Rodriguez, J. D. Barnes, G. B. McKenna, *Langmuir* **1994**, *10*, 3406–3418.

Received: August 25, 2009
Published online: January 29, 2010

